Models for control of intravenous anesthesia

Soltesz, Kristian; van Heusden, Klaske; Dumont, Guy A.

Published in:
Automated drug delivery in anesthesia

DOI:
10.1016/B978-0-12-815975-0.00010-2

2020

Document Version:
Early version, also known as pre-print

Models for control of intravenous anesthesia

Kristian Soltesz[1] **Klaske van Heusden**[2] **Guy A. Dumont**[3]

[1]*Lund University, Dept. of Automatic Control*
[2]*University of British Columbia, Dept. of Electrical and Computer Engineering*
[3]*Corresponding: kristian@control.lth.se*

Abstract: Modeling is fundamental to both feed-forward and feedback control. Within automated anesthesia the two paradigms are usually referred to as target-controlled infusion (TCI) and closed-loop drug delivery, respectively. In both cases, the objective is to control a system with anesthetic drug infusion rate as input, and (measured) clinical effect as output. The input is related to the output through the pharmacokinetics (PK) and pharmacodynamics (PD) of the patient. This chapter gives an introduction to PKPD modeling in automated anesthesia management, intended to be accessible to both anesthesiology and (control) engineering researchers. The following topics are discussed: the role of modeling; the classic PKPD structure used in clinical pharmacology; anesthesia modeling and identification for closed-loop control; inter-patient variability and model uncertainty; disturbance, noise and equipment models. The chapter emphasizes electroencephalogram-guided control of propofol.

1. Introduction

This section introduces the scope of this chapter in Section 1.1, whereupon the disposition of the material follows in Section 1.2.

1.1 Scope

This chapter introduces model structures commonly used to describe patient dynamics in anesthesia. While early research on closed-loop controlled anesthesia, such as [Soltero et al., 1951], considered volatile anesthetics, the introduction and increased popularity of total intravenous anesthesia (TIVA) [Absalom and Kiera, 2017] has heavily shifted focus of the anesthesia control research community toward modeling and control of intravenously induced and maintained anesthesia [Le Guien et al., 2016]. Relatedly, most automatic drug delivery research in anesthesia has focused on controlling the hypnotic component of anesthesia through closed-loop controlled titration of propofol, based on measurements from an electroencephalogram (EEG) monitor. A partial overview of works on EEG-controlled propofol infusion can be found in [Le Guien et al., 2016; Neckebroeak et al., 2013].

Several attempts have also been made to control the analgesic component of anesthesia, foremost using fast opioids such as remifentanil. Analgesia control is complicated by the absence of reliable nociception monitors with wide clinical acceptance [Gruenewald and Ilies, 2013]. Monitors utilizing individual measurements have been reported to suffer from low specificity, as exemplified in [Choo et al., 2010]. Consequently, associated control research has focused on developing new measurement techniques [Jeanne et al., 2009; Chevalier et al., 2014] and in estimating the level of analgesia using (sometimes model-based) sensor fusion approaches utilizing already monitored variables, as in for example [Merigo et al., 2019; van Heusden et al., 2018b; Guignard, 2006; Huiku et al., 2007; Hemmerling et al., 2009].

There exist several works, such as [Zhanybai et al., 2015; Mendonça et al., 2004], on modeling and control of neuromuscular blockage using rocoronium or other muscle relaxants. Most commonly, the train-of-four (ToF) [Lee, 1975] measurement is used as feedback variable in this context. Control

[1] Parts of the material in this chapter has previously been published in [Soltesz, 2013] ©Kristian Soltesz.

of neuromuscular blockage is particularly tractable as there are generally no exogenous disturbances from for example drug interaction or surgical stimulation.

As a consequence of the above, the content of this chapter focuses on modeling for EEG-controlled propofol infusion. The introduced model structures, principles and discussions are, however, applicable to all three components of anesthesia, and to a large extent also apply in the context of volatile anesthetics. With this in mind, the chapter should be viewed as an introduction to aspects of modeling relevant to control, rather than an exhaustive review of the field.

1.2 Disposition

The chapter is divided into two main sections. Section 2 introduces the model structures traditionally used within clinical physiology to describe pharmacokinetics (Section 2.2) and pharmacodynamics (Section 2.3). The chapter is opened with a discussion on the purpose for which these models were introduced, mostly prior to the advent of closed-loop anesthesia systems. Models of the pharmacodynamic interaction between hypnosis (propofol) and analgesia (remifentanil or other opioids) are reviewed in Section 2.5. The section is concluded with a discussion in Section 3.2, on how individual and population parameters for the above model structures have been obtained from clinical data.

In Section 3, focus is shifted to models for closed-loop control. Desired model properties are presented in Section 3.1. Section 3.2 discusses problems of identifiability associated with clinical data. It is followed by Section 3.3, dedicated to modeling for control. Variability in dynamics, particularly between individual patients of a population, is the topic of Section 3.4. Approaches to arrive at linear model representations, despite the presence of a nonlinear component (the Hill function introduced in Section 2.3) are presented in Section 3.5. Finally, the dynamics of monitoring and actuation equipment, and of exogenous disturbances, are discussed in Section 3.6.

2. Models from clinical pharmacology

This section presents modeling concepts originating from clinical pharmacology. The purpose, which the resulting models were intended to fill is described in Section 2.1. Subsequently, pharmacokinetics are introduced in Section 2.2, followed by pharmacodynamics in Section 2.3. Their combination, the PKPD model, is summarized in Section 2.4. Section 2.5 introduces structures to model pharmacodynamic interaction between drugs. Finally, a few remarks on how parameter values are typically identified for (population) PKPD models, are provided in Section 2.6.

2.1 The purpose of modeling

In clinical anesthesia, models are used on a daily basis in operating rooms around the world, directly or indirectly. They are the basis of drug dosing recommendations, dosing schemes and computer controlled (feed-forward) infusion systems, referred to as target controlled infusion (TCI) systems [Absalom and Kiera, 2017]. Derived concepts such as context-sensitive half-time (explained further below) are important in the clinicians' mental model, allowing them to provide accurately titrated intravenous anesthesia.

Intravenous drugs used for general anesthesia include hypnotic agents, analgesic agents and muscle relaxants. The goal of anesthesia during surgery (and largely applicable also to anesthesia for investigation and long-term intensive care scenarios) is to rapidly induce unconsciousness and avoid awareness during the operation, to titrate analgesia to avoid responses to nociceptive stimulation while maintaining hemodynamic stability, and to facilitate rapid recovery. This cannot be achieved with constant infusion rates; bolus or loading doses are given to rapidly induce anesthesia, and the anesthesiologist continues to adjust drug dosing during the case and can administer bolus doses in anticipation or response to stimulation. In anticipation of the end of surgery, drug dosing adjustments can be made to ensure rapid recovery. To achieve this, understanding of the time course of the drug effect is essential [Minto and Schnider, 2008].

Pharmacokinetics and pharmacodynamics study this time course of the drug effect: pharmacokinetics (PK, further explained in Section 2.2) describe what the body does to the drug, i.e., how it is distributed and eliminated; pharmacodynamics (PD, further explained in Section 2.3) describe what the drug does to the body, i.e., how the clinical effect is related to the drug concentration. Their combination, the PKPD modeling of anesthetic agents, has therefore attracted a lot of attention. Figure 1 shows the simulated time evolution of the blood plasma drug concentration (left) and clinical effect

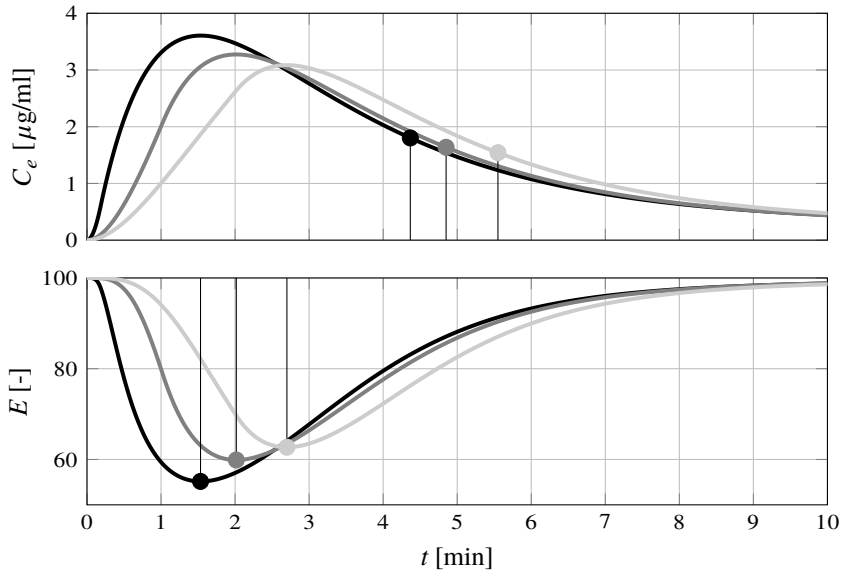

Figure 1 Effect-site concentration (top) and effect (bottom), following a propofol bolus of 1 mg given over 10 s (black), 20 s (dark gray) and 30 s (light gray), and starting at $t = 0$. Context-sensitive half-time is marked in the top plot; (time to) peak effect in the bottom. The concentration responses were obtained by simulating the Schnider PK model and associated effect-site PD [Schnider et al., 1998] for a female patient, weighing 60 kg, being 30 years old and 165 cm tall. The PD parameters, with definitions below in Section 2.3, were $C_{e,50} = 4$ μg/ml and $\gamma = 2$. Effect is reported using the BIS scale, with $E_0 = 100$; $E_{\max} = 0$.

(right), following a propofol bolus of 1 mg at $t = 0$. The figure illustrates time-to-peak effect and context-sensitive half-time, being two parameters frequently used by clinicians.

Rational selection of anesthetic agents and dosing has thus been made possible by PKPD modeling and the development of derived concepts [Lemmens and Stanski, 2012].

Understanding of the onset of drug effect is important in clinical anesthesia. To accommodate observed time delays between intravenous drug delivery and drug effect (not visible in the simulation outcome of Figure 1), the effect-site concept was introduced [Sheiner et al., 1979]. It allowed for modeling of dynamics relating the plasma concentration and the observed effect, without affecting the drug mass in the PK model, as further discussed in Section 2.3. The effect-site model has been used to optimize bolus doses and to determine equipotent bolus doses for different drugs [Minto and Schnider, 2008]. The time-to-peak effect, illustrated in Figure 1, combines PK and PD characteristics and directly compares onset times [Gambús and Trocóniz, 2015]. Recovery following drug delivery is strongly influenced by the duration of drug administration, and has led to the introduction of the term “context-sensitive half-time” (where the context is defined by the drug infusion profile). The context-sensitive half-time cannot be explained by drug elimination rates alone, and simulation of decreasing plasma concentrations using PKPD models offered more realistic predictions of recovery [Shafer and Varvel, 1991].

PK models have been used to derive manual infusion schemes for adults (for example [Roberts et al., 1988]). Subsequently, computer controlled TCI systems were developed that explicitly use the PK and PD models and calculate an optimal (feed-forward) drug infusion trajectory to achieve a desired target plasma or effect-site concentration [Absalom and Kiera, 2017]. Two commercially available clinical decision support systems explicitly use PKPD models to visualize real-time concentrations as calculated by the models, and incorporate predictions of future values (Navigator Applications Suite, GE Healthcare, USA; SmartPilot View, Dräger, Germany).

To conclude, the development of dynamic models in anesthesia have been driven by pharmacological needs associated with manual drug administration. The main use of models has been to capture slow phenomena, such as time-to-peak effect following a bolus, (contextual) half-time of drugs and the steady-state clinical effect associated with a given constant drug infusion rate for a particular patient. While the resulting models have proven useful for drug dose recommendations, their properties are not necessarily the ones required for the synthesis of feedback controllers, as further

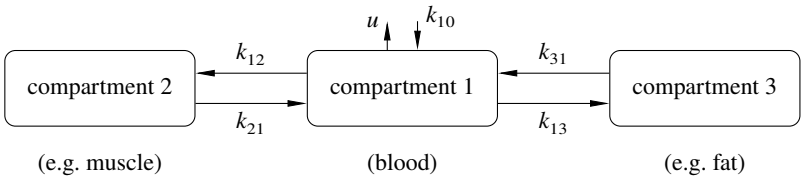

Figure 2 A mammillary compartment model with three compartments. Drug flow between compartments is governed by rate constants k_{ij}. Elimination to the environment (compartment) is governed by k_{10} and drug is introduced to the central compartment with infusion rate u.

discussed in Section 3.

2.2 Pharmacokinetics

The traditional model structure used to describe the PK of a particular drug is the mammillary compartment model, schematically illustrated in Figure 2. The number of compartments required to capture response dynamics vary between drugs. For instance, clinical models for propofol typically have three compartments, as in [Sahinovic et al., 2018]. The two most widely utilized PK models for remifentanil have respectively two and three compartments [Minto et al., 1997; Rigby-Jones et al., 2007].

Drug mass in compartment i is denoted $m_i \geq 0$ and the per time proportion of drug migrating from compartment i to j is described by the rate constant $k_{ij} \geq 0$:

$$\dot{m}_i = \sum_{j=1}^{n} k_{ji} m_j - \sum_{j=0}^{n} k_{ij} m_i + u_i, \tag{1}$$

where n is the number of compartments in the model. The compartment corresponding to $i = 0$ is the environment and k_{j0} models elimination of drug from compartment j. The per time mass of drug introduced into compartment i from the environment is described by $u_i \geq 0$. The system of equations defined through (1) constitutes a delay-free linear and time-invariant (LTI) system [Rugh and Kailath, 1995].

In the context of intravenous anesthesia, the central compartment represents the blood, being the site where drug is introduced. Consequently $u_i = 0 \; \forall i \neq 1$ and it is natural to introduce $u = u_1$. The peripheral compartments only exchange drug with each other indirectly through the central compartment, as shown in Figure 2. Furthermore, drug is assumed only to be eliminated from the central compartment. In the intravenous context, such elimination is typically through metabolism in the liver, combined with renal excretion [Bryson et al., 1995]. In the volatile context, some of the elimination is also attributed to pulmonary gas exchange.

The compartment model illustrated in Figure 2, and governed by (1), has the following state space representation:

$$\dot{m} = \begin{bmatrix} -(k_{10} + k_{12} + k_{13}) & k_{21} & k_{31} \\ k_{12} & -k_{21} & 0 \\ k_{13} & 0 & -k_{31} \end{bmatrix} m + \begin{bmatrix} 1 \\ 0 \\ 0 \end{bmatrix} u, \tag{2}$$

where $m = [m_1 \; m_2 \; m_3]^T$ is the state vector. It is straightforward to derive state space equations for a compartment system of arbitrary order and topology. However, increasing the parameters also increases demands on clinical identification data, in order to avoid over-fitting. For practical purposes, the three-compartment system is generally sufficient to model pharmacokinetics of anesthetic drugs. For some anesthetic drugs, particularly opioids, two compartments are sufficient to model pharmacokinetics. The two-compartment model constitutes a special case of (2), and is consequently not explicitly presented here.

In order for (2) to be a realistic model, it is necessary that there is no net flow between compartments i and j, whenever they hold the same drug concentrations, i.e., $x_i = x_j$, where

$$x_i = \frac{m_i}{v_i}. \tag{3}$$

In (3), x_i is the drug concentration in compartment i, which has volume v_i. Note that the compartment volumes, also referred to as volumes of distribution, are a theoretical construct and should not

be thought of in terms actual physiological volumes. (For instance, many drug PK models involve compartments of volumes exceeding that of the human body.) The mentioned net flow constraint can now be states, assuming equal concentrations $x_i = x_j$:

$$k_{ji}m_j = k_{ij}m_i \quad \Leftrightarrow \quad k_{ji}v_jx_i = k_{ij}v_ix_j \quad \Leftrightarrow \quad k_{ji}v_j = k_{ij}v_i. \tag{4}$$

Combining (1) and (4) yields

$$\begin{aligned} \frac{1}{v_i}\dot{m}_i &= \sum_{j=1}^{n}\frac{v_j}{v_i}k_{ji}\frac{m_j}{v_j} - \sum_{j=0}^{n}k_{ij}\frac{m_i}{v_i} + \frac{1}{v_i}u_u \\ \Leftrightarrow \qquad \dot{x}_i &= \sum_{j=1}^{n}\frac{v_j}{v_i}k_{ji}x_j - \sum_{j=0}^{n}k_{ij}x_i + \frac{1}{v_i}u_i \\ \Leftrightarrow \qquad \dot{x}_i &= \sum_{j=1}^{n}k_{ij}(x_j - x_i) - k_{i0}x_i + \frac{1}{v_i}u_i. \end{aligned} \tag{5}$$

Note that the compartment volumes only enter (5) as an input scaling. Consequently, the model (5) is fully parameterized by $k_{10}, k_{12}, k_{13}, k_{21}, k_{31}$ and v_1 (6 parameters) in the three compartment case and by k_{10}, k_{12}, k_{21}, and v_1 (4 parameters) in the two compartment case. The state space representation corresponding to (2) becomes

$$\dot{x} = \begin{bmatrix} -(k_{10}+k_{12}+k_{13}) & k_{12} & k_{13} \\ k_{21} & -k_{21} & 0 \\ k_{31} & 0 & -k_{31} \end{bmatrix} x + \begin{bmatrix} \frac{1}{v_1} \\ 0 \\ 0 \end{bmatrix} u. \tag{6}$$

It could be noted here that both (2) and (6) are positive systems, since their system matrices are of Metzler type. However, only (6) is guaranteed to describe a compartmental system [Luenberger, 1979].

Assuming the plasma concentration $C_p = x_1$ is the output of (6), the system has the following transfer function representation

$$G_{C_p,u}(s) = \frac{1}{v_1}\frac{(s+k_{21})(s+k_{31})}{(s+p_1)(s+p_2)(s+p_3)}. \tag{7}$$

In (7) the Laplace variable s constitutes the Laplace transform of the differential operator $\partial/\partial t$. The curious reader without a control system background is referred to a standard text on linear systems, such as [Rugh and Kailath, 1995] for a further explanation. The poles $-p_i$ in (7) solve the characteristic equation

$$\begin{cases} p_1 + p_2 + p_3 = k_{12}0k_{13} + k_{21} + k_{31} \\ p_1p_2 + p_1p_3 + p_2p_3 = k_{10}(k_{21}+k_{31}) + k_{31}(k_{12}+k_{21}) + k_{13}k_{21} \\ p_1p_2p_3 = k_{10}k_{21}k_{31}. \end{cases}$$

In some literature, the PK model is parametrized in terms of the clearance c_i, describing the drug volume per time, migrating from a specific compartment. The clearances for the system (6) are:

$$\begin{cases} c_1 = v_1k_{10} \\ c_2 = v_2k_{21} = v_1k_{12} \\ c_3 = v_3k_{31} = v_1k_{13}, \end{cases}$$

where the rightmost equalities follow from (4).

The system model (6) or (7) uniquely determines the time evolution of drug concentration in each compartment given a known initial condition (for example $x = 0$ at $t = 0$, where $t = 0$ marks the beginning of infusion), and an infusion profile $u(t)$, where $t \geq 0$. Consequently, it can be used to compute clinically relevant properties such as time-to-peak concentration, peak concentration resulting from a particular infusion profile and (context-sensitive) half-time. This is achieved using well-established methods for linear systems, presented in for example [Rugh and Kailath, 1995].

A related approach to the compartment model formulation stated above, is the use of fractional order models. Such models typically arise as the solution to diffusion problems, and their use in the pharmacokinetic modeling context can be motivated by this, i.e., by diffusion of drug between compartments. The reader is referred to [Ionescu et al., 2017] for a thorough introduction.

2.3 Pharmacodynamics

This section introduces the model structures classically used to describe pharmacodynamics. They comprise an input component, described in Section 2.3, in series with an output component, described in Section 2.3.

Effect dynamics The classical PD relates the clinical effect, E, to the plasma drug concentration, C_p. In controlling the the hypnotic component of anesthesia, the depth of hypnosis (DoH) is the considered clinical effect, E. The two will be used interchangeably henceforth, unless some other endpoint, such as nociception, is explicitly considered. It is possible to track C_p in (7) by drawing time stamped blood samples, which are subsequently analyzed. (The practically achievable bandwidth of this methodology is not sufficient for closed-loop control purposes, but useful for identification of the PK model parameters.) When comparing the measured blood plasma concentration from such blood samples to monitored clinical effect, some drugs, including the hypnotic agent propofol, yield a lag, which is not accounted for by the dynamics of the monitor. A contributing reason to this is that the dynamics between the blood plasma and the effect site, which for propofol is the cerebellar cortex, are not modeled. It was suggested in [Sheiner et al., 1979], and confirmed in [Absalom and Kiera, 2017], that the PD model (7) should be augmented by a series connected lag link

$$G_{C_p,C_e} = \frac{k_{e0}}{s + k_{e0}}, \tag{8}$$

at its input, where C_e is referred to as the effect-site concentration of the drug. Introducing the notation $x_e = C_e$ for the effect-site concentration, the state space representation of (8) becomes

$$\dot{x}_e = -k_{e0}x_e + k_{e0}x_1, \tag{9}$$

where x_1 is the primary compartment drug concentration. From the notation of (9) it appears as if x_e is the drug concentration in a compartment, which is fed by the central compartment, and from which drug is eliminated to the environment by a rate constant k_{e0}. Assuming this "effect-site compartment" holds drug mass m_e and has volume v_e, its dynamics are described by

$$\begin{aligned} & \dot{m}_e = -k_{e0}m_e + k_{1e}m_1 \\ \Leftrightarrow \quad & \frac{1}{v_e}\dot{m}_e = -k_{e0}\frac{m_e}{v_e} + \frac{v_1}{v_e}k_{1e}\frac{m_1}{v_1} \\ \Leftrightarrow \quad & \dot{x}_e = -k_{e0}x_e + k_{e1}x_1, \end{aligned} \tag{10}$$

where the last equivalence follows from (4). Equating (9) with (10) yields $k_{e0} = k_{e1}$. However, to fit into the compartment framework, a term $-k_{1e}x_1$, describing the drug flow from the central compartment to the effect-site compartment, would have to be added to the dynamics of $\dot{x}_1$ in (6). Since $k_{1e} = v_e/v_1 \cdot k_{e1}$, it follows that $k_{1e} \approx 0$ when $v_e \ll v_1$. Consequently, the effect-site model (8) fits into the compartment framework under the realistic assumption that the effect-site compartment has negligible volume compared to the central compartment. Under this assumption it also becomes irrelevant whether the term $-k_{e0}x_e$ in (8) corresponds to elimination of drug to the environment or reflux to the central compartment. The latter would add the influx term $k_{1e}x_e$ to the dynamics of $\dot{x}_1$ in (6), which is negligible if $k_{e1} \approx 0$.

Later, it has been suggested that the effect-site model should be augmented by a series connected time delay [Bibian, 2006], as further discussed in Section 3.3.

The Hill sigmoid The common definition is that the PD relates the clinical effect, E, to the blood plasma drug concentration, C_p. If the effect-site compartment of Section 2.3 is employed, as will be the case herein, it instead relates E to the effect-site concentration, C_e. The role of the PD (other than the effect dynamics) is to account for the nonlinear static relation between C_e and E.

The clinical effect, E, is typically reported on a scale between 100 and 0, where $E_0 \approx 100$ represents the effect in absence of drug (when $C_e = 0$) and $E_{\max} \approx 0$ represents the maximally achievable effect (for large C_e). The concentrations yielding $E = 50$ is denoted $C_{e,50}$. In contexts where $E_0 \neq 100$ or $E_{\max} \neq 0$, $C_{e,50}$ can alternatively be defined as the concentration yielding $E = \frac{1}{2}|E_{\max} - E_0|$. It should be noted that values of E_0, $C_{e,50}$ and $E_{\max}$ are patient-specific.

While the 100-0 scale can be confusing to the control engineer (any linearization of the process dynamics will have negative steady state gain), it is what clinicians are used to, and what is reported

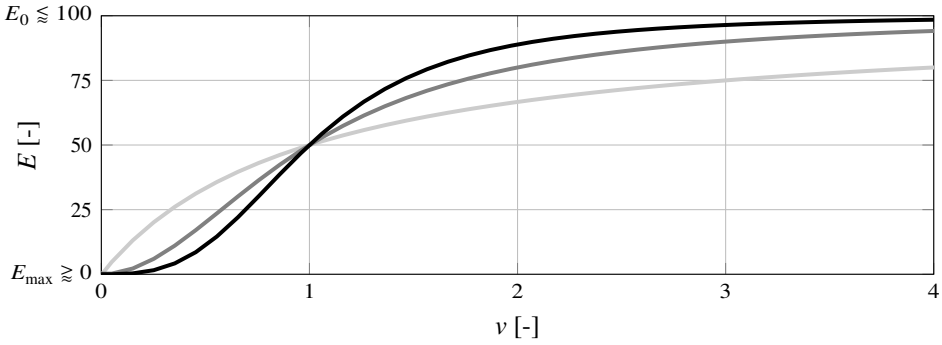

Figure 3 The Hill function, parameterized in γ, defines the clinical effect E in terms of normalized effect-site concentration $v = C_e/C_{e,50}$. Here curves for $\gamma = 3$ (black), $\gamma = 2$ (dark gray) and $\gamma = 1$ (light gray) are shown. Effect is reported using the BIS scale, with $E_0 = 100$; $E_{\max} = 0$.

by clinical monitors. The scale is often referred to as the "BIS" scale, after the BIS monitor (Aspect Medical Systems, USA), and has been used by other DoH indices such as the WAV_{CNS} reported by the NeuroSense monitor (Neurowave Systems, USA). For control system analysis and synthesis purposes, it can be convenient to instead work with the normalized effect

$$\bar{E} = \frac{E - E_0}{E_{\max} - E_0} -$$

In this chapter DoH and E will be used interchangeably, and reported on the BIS or WAV_{CNS} scales. For control synthesis purposes it is straightforward to map the range $E_0 - E_{\max}$ to $0 - 1$ by means of an affine transformation:

$$\bar{E} = \frac{E - E_0}{E_{\max} - E_0}. \tag{11}$$

The default choice for the structure of $E(C_e)$ in the literature is the Hill function (also known as the sigmoidal Emax function):

$$E(t) = E_0 - (E_0 - E_{\max})\frac{C_e(t)^\gamma}{C_e(t)^\gamma + C_{e,50}^\gamma}, \qquad \gamma \geq 1. \tag{12}$$

The definition of E_0 and $E_{\max}$ varies between publications, which needs to be kept in mind when working with published parameter values. For instance [Ionescu et al., 2008] uses a slightly different definition. The one in (12), used also in for instance [Minto et al., 2000], is motivated by the intuitive the steady state relations $C_e = 0 \;\Rightarrow\; E = E_0$ and $C_e \to \infty \;\Rightarrow\; E = E_{\max}$.

The Hill equation (12) can also be expressed in the normalized effect-site concentration, v,

$$E(t) = E_0 + (E_{\max} - E_0)\frac{v^\gamma}{1 + v^\gamma}, \qquad v = \frac{C_e}{C_{e,50}}, \quad \gamma \geq 1. \tag{13}$$

The parameter γ is referred to as the Hill parameter or Hill degree. The Hill function, for three values of γ, is shown in Figure 3.

From clinical data it is hard to argue that there is no model structure better for the task than (12). However, the Hill function (closely related to the logistics function) is structurally simple and features characteristics which are observed in clinical practice: it has a linear region around $C_e = C_{e,50}$ and saturation effects as $C_e \to 0$ and $C_e \to \infty$, respectively. For some drugs, the use of the Hill function can be motivated by ligand binding models from receptor theory [Derendorf and Meibohm, 1999].

2.4 The PKPD model structure

Combining the PK of Section 2.2 with the PD of Section 2.3 yields the combined PKPD model structure, schematically illustrated by the block digram of Figure 4. The PKPD model of Figure 4 is an LTI system with a static output nonlinearity. As such, it constitutes a Wiener model [Ljung, 1999] comprising the LTI input model of (7),

$$G_{C_p,u}(s) = \frac{1}{v_1}\frac{(s + k_{21})(s + k_{31})}{(s + p_1)(s + p_2)(s + p_3)},$$

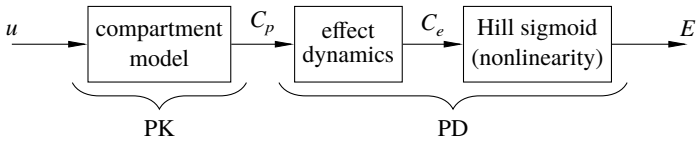

Figure 4 Block diagram illustrating the PKPD structure used in clinical pharmacology. It is divided into a pharmacokinetics (PK) model, in series connection with a pharmacodynamics (PD) model. The PK is modeled using a mammillary compartment model, being a special case of a linear and time-invariant (LTI) system. It relates blood plasma drug concentration, C_p to drug infusion rate, u. The PD has en LTI input part, relating effect-site concentration, C_e, to C_p through a first-order lag (with delay). It is followed by a static sigmoidal nonlinearity, relating to clinical effect, E, to C_e.

in series with the Hill sigmoid

$$E(t) = E_0 + (E_{\max} - E_0)\frac{C_e(t)^\gamma}{C_e(t)^\gamma + C_{e,50}^\gamma}, \qquad \gamma \geq 1$$

of (12).

When PKPD modeling is mentioned in the context of drug delivery in anesthesia, it typically refers to this structure (unless otherwise stated).

2.5 Pharmacodynamic interaction

While there is no significant PKPD interaction between commonly utilized neuromuscular blocking agents and other anesthetic agents, it is well-known that several hypnotic and analgesic agents interact synergistically both toward loss of awareness and nociception. Notably, the hypnotic agent propofol exhibits a synergistic interaction with analgesics from the opioid family, such as fentanyl and remifentanil.

In clinical practice the synergy results in a propofol sparing effect when remifentanil (or another opioid) is co-administered. A dose-dependent effect of this kind was for instance observed in a study where propofol administration was controlled in closed-loop, based on auditory evoked potentials [Milne et al., 2003]. Remifentanil was shown to decrease the propofol $C_{e,50}$ for response to stimulation [Drover et al., 2004]. This occurred at relatively low doses and higher doses did not increase interaction.

The PK of propofol is not affected by remifentanil co-administration, and the effect of propofol on the remifentanil PK is only relevant when propofol is administered as bolus [Bouillon et al., 2002]. Consequently, the synergy is attributed to the PD. In the control engineering community, studies of interaction effect have mostly focussed on the effect toward hypnosis. However, effects toward analgesia are also of clinical importance. For example, probability of sedation measured according to the "observer assessment of alertness/sedation score", probability of response to laryngoscopy, level of tolerated tetanic stimulus and level of tolerated algometry pressure, as quantified in [Kern et al., 2004]. Results from such drug interaction studies allow clinicians to optimize drug combinations and dosing, to achieve the desired effect while minimizing side effects. An interaction model is explicitly used in the SmartPilot View clinical monitor (Dräger, Germany); a two-dimensional visualization of drug concentrations which includes isoboles reflecting the probability of response to painful stimuli.

Synergy is commonly modeled using a generalization of the Hill curve to a surface. I.e., the hypnotic effect, E_h, becomes a function of the normalized propofol (subscript p) and remifentanil (subscript r) effect-site concentrations:

$$E_h = E_h(v_p, v_r), \tag{14}$$

where v_r is defined in the same way as $v = v_p$ was in (13). Different parametric structures have been suggested for (14). The most common one found in the literature is the one presented in [Minto et al.,

2000]:

$$E_h(v_p, v_r) = E_0 + (E_{\max}(\theta) - E_0)\,\frac{\left(\frac{v_p + v_r}{v_{50}(\theta)}\right)^{\gamma(\theta)}}{1 + \left(\frac{v_p + v_r}{v_{50}(\theta)}\right)^{\gamma(\theta)}} = E_0 + (E_{\max}(\theta) - E_0)\,\frac{1}{1 + \left(\frac{v_p + v_r}{v_{50}(\theta)}\right)^{-\gamma(\theta)}} \tag{15}$$

where θ is the relative concentration:

$$\theta = \frac{v_r}{v_p + v_r}.$$

An interpretation of this parametrization is that $v_p + v_r$ is the concentration of a virtual drug with $C_e/C_{e,50} = v_{50}(\theta)$. This virtual drug has a Hill-like PD, where the Hill coefficient γ (and the maximal effect, $E_{\max}$) also potentially depend on the relative concentration, θ. It was suggested in [Minto et al., 2000] that a fourth-order polynomial be used to model $v_{50}(\cdot)$ and a second-order one for $\gamma(\cdot)$. The interaction surface is defined through the coefficients of these polynomials, which need to be identified from clinical data. An interaction plane, being a local linearization of the interaction surface (15) was proposed in [Ionescu et al., 2011a].

Another parametrization for the interaction surface was proposed in [Kern et al., 2004]. It constitutes an extension of (12), where v denotes relative concentration of the virtual drug

$$v = \max(v_p + v_r + \alpha v_p v_r, 0). \tag{16}$$

The structure (16) has only one parameter, α. Another appealing feature is that the interaction model exactly corresponds to the propofol PD in the absence of remifentanil ($v_r = 0 \Rightarrow v = v_p$). Values of α toward different effects have been published in [Kern et al., 2004].

A third example of interaction model, proposed to model the response to propofol and remifentanil co-administration is presented further below in (20) of Section 3.3.

2.6 Parameter identification

Individual responses to drug infusion are highly variable. The population approach in PKPD modeling quantifies the population mean dynamics, as well as inter-patient variability [Sheiner and Beal, 1980]. Nonlinear mixed-effect modeling (NONMEM) [Sheiner et al., 1977] is the gold standard in pharmacology for identifying such models from data. NONMEM simultaneously optimizes over population average models, inter-patient variability and intra-patient variability. It can be used for sparse data, i.e. modeling can be done from data sets with few samples per individual. It incorporates fixed effects from user-defined covariates in the inter-patient variability [Heeremans et al., 2010]. Identification of covariates such as age, weight etc. allows for personalization of anesthetic drug dosing, i.e. drug dosing that takes patient demographics known to affect pharmacokinetics or dynamics into account.

Clinical data used to develop models for clinical pharmacology are often collected in volunteer studies, for example [Schnider et al., 1999], or using modeling-specific protocols during a surgical procedure, for example [Cortinez et al., 2010]. In these studies, drug dosing may be varied with limited clinical constraints, while of course maintaining patient safety. Step-wise changes in drug dosing are used to characterize the response to different drug levels and to characterize nonlinear behavior. Different levels may be targeted in different volunteer subjects. These experiments can be designed specifically for the modeling purpose, and blood samples can be taken for modeling the PK characteristics. Blood samples drawn after drug infusion is stopped provide valuable information for elimination and for parameter identification of a third compartment (see Figure 2).

The two PKPD models most widely used in TCI for propofol are the Schnider and the (modified) Marsh model [Absalom et al., 2009]. The Schnider model was identified from data from a volunteer study [Schnider et al., 1998; Schnider et al., 1999]. Volunteers received a rapid bolus of propofol, no drug infusion for 60 minutes, followed by a constant 60 minute infusion. Infusion rates were randomly assigned to 25, 50, 100 or 200 μg/kg/min, with two patients per group. Arterial blood samples were drawn at the following times after the start of the propofol bolus: 0, 1, 2, 4, 8, 16, 30, 60, 62, 64, 68, 76, 90, 120, 122, 124, 128, 136, 150, 180, 240, 300 and 600 minutes.

The PD model was derived from an EEG-based measure of DoH. PK model validation indicated a reasonable model fit during constant infusion and during recovery. However, the model fit following the bolus and infusion rate changes was limited and indicates bias [Schnider et al., 1998]. Note that this data set includes only 3 samples during the expected duration of induction of anesthesia (1, 2, and 4 minutes following the bolus). This sparsity of data also limits model reliability when used in a closed-loop context, with a reasonably fast closed-loop bandwidth. A fixed $k_{e0} = 0.459$ min^{-1} was identified in combination with this PK model [Schnider et al., 1998]. The observed time-to-peak effect ranged from 1 to 2.4 minutes.

The Marsh model [Marsh et al., 1991] was adjusted from the Gepts model [Gepts et al., 1987]. Eighteen patients received constant propofol infusion of 3, 6, or 9 mg/kg/hr during surgery requiring regional anesthesia. Blood samples were drawn at 2, 4, 6, 8, 10, 20, 30, 40, 50, 60, 75, 90, 105 and 120 minutes after the start of propofol infusion, as well as 2, 4, 6, 8, 10, 20, 40, 60, 90, 120, 180, 240, 300, 360, 420, and 480 minutes after propofol infusion was stopped. As with the Schnider model, sparsity of data is expected to limit model reliability in the dynamic range of primary interest for closed-loop control. Complete details for the Marsh model adjustments [Marsh et al., 1991] have not been published [Absalom et al., 2009]. A pharmacodynamic time constant of $k_{e0} = 0.26$ min^{-1} has been used in combination with this model, while $k_{e0} = 1.2$ min^{-1} was proposed to better reflect a time-to-peak effect of 1.6 minutes [Struys et al., 2000], also referred to as the modified Marsh model [Absalom et al., 2009].

The drug distribution following a bolus dose is not well characterized by compartmental models [Cortinez, 2014], which is reflected in the poor model fit following the bolus and rate changes [Schnider et al., 1998], as discussed above. There are discrepancies between published models [Cortinez, 2014]. The two models commonly used, the Schnider and Marsh model, are also known to differ, particularly during bolus or TCI induction of anesthesia. In manual and feed-forward control, this needs to be taken into account [Absalom and Struys, 2007].

When using the Marsh model during TCI induction of anesthesia, a target concentration of 3 mg/ml may provide an adequate induction bolus, while an initial target of 5 mg/ml is more commonly used for the Schnider model, reduced to 3 mg/ml after $\approx$ 10 minutes [Absalom and Struys, 2007]. The low-frequency and steady-state characteristics are similar, resulting in similar TCI infusion rates during maintenance of anesthesia.

Inter-patient variability to propofol infusion remains a limiting factor for feed-forward (TCI) drug administration. PKPD modeling studies aiming at improving models for specific target populations are ongoing, for example [Diepstraten et al., 2012], as well as studies evaluating the accuracy of published models in target populations, for example [Cortínez et al., 2014; Hara et al., 2017]. Aggregated data from clinical studies in several target populations have been used to identify a population PK model for a range of patient groups and conditions [Eleveld et al., 2014]. Cumulative optimal doses calculated based on this new model are similar to models currently used in TCI, and inter-patient variability that was not explained by the covariates remained high, particularly in patients with high body mass index [Eleveld et al., 2014]. A review of propofol and remifentanil models obtained using classical pharmacological techniques is available in Appendix B of [Bibian, 2006].

3. Models for control

The purpose of this section is to discuss models, which have been developed particularly for feedback control. Section 3.1 outlines the purpose of such models, and some of the challenges associated with obtaining them. Representative properties of clinical data available for online modeling are discussed in Section 3.2. Section 3.3 provides snapshots of published strategies for obtaining models specifically for the purpose of feedback control. Patient variability and its modeling is the topic of Section 3.4. Section 3.5 is dedicated to techniques for linearizing the Hill function introduced in Section 2.3, in order to enable controller synthesis techniques relying on LTI process representations (as most are). Finally, aspects of modeling of everything in the control loop except the actual patient, is considered in Section 3.6.

3.1 The purpose of modeling

In the development of an automated system for intravenous anesthesia delivery, the goal of deriving patient models is to design a closed-loop controller. Design specifications include the target popu-

lation and clinical objectives that may depend on the procedure as well as the characteristics of the patient. For example, during endoscopic investigations spontaneous breathing needs to be maintained, while in many other procedures rapid induction of anesthesia is required to ensure timely airway instrumentation to avoid hypoxia. In elderly patients, rapid induction of anesthesia may compromise hemodynamic stability and slower induction may be preferred.

Any automated system will have to meet performance and safety criteria for all patients in the target population. No information about the specific patient other than demographics (age, weight etc.) and medical history is typically known prior to the use of the system, and while experiments for individual model development may be performed in the context of a clinical study, such experiments cannot be performed in clinical practice prior to surgery. Any online modeling or model individualization is therefore restricted to data collected during surgery, i.e. data from induction and maintenance of anesthesia.

The above-mentioned conditions are routinely dealt with when performing manual or TCI anesthesia in the operating room. However, in closed-loop anesthesia, the automated system will update the drug infusion at a much higher rate than associated with manual dosing. Population PKPD models were developed for manual or TCI drug dosing, and population average characteristics such as time-to-peak effect, low-frequency gains, and context-sensitive half-times are important to developing a mental model for manual control, and TCI strategies targeting constant effect concentrations, respectively. However, for closed-loop control, low-frequency characteristics do not have to be described accurately as the controller will achieve disturbance rejection within the closed-loop bandwidth (for instance through integral action) [Åström and Murray, 2008]. Instead, the closed-loop characteristics and performance achieved by the to-be-designed controller are what really matters, not the model or its characteristics [Gevers, 2005].

It is now well-known that models for control need to be accurate around the closed-loop bandwidth. Optimal models for control therefore depend on the controller to be designed, which is unknown at the time of modeling [Gevers, 2005]. Iterative modeling and control methods have been proposed [Lee et al., 1993] as well as approximations that do not require iterations [Hjalmarsson, 2005]. When identifying a model for control from data, a well-designed experiment can improve controller performance [Gevers, 2005]. Modeling to accurately predict closed-loop characteristics has been studied extensively [Gevers, 2005].

When model-based controller design methods were developed in the 1960s, models derived from data were used, and it was assumed that they adequately represented the true system. However, when applied to complex systems, this led to failures as robustness considerations were not taken into account [Safonov, 2012]. The consequent shift to robust control required modeling tools that provide both a model and an uncertainty description [Gevers, 2005]. Methods to derive control-oriented nominal models and associated uncertainty sets were consequently developed [Gevers, 2005].

Most results in the mentioned field of modeling and identification for control focus on linear systems or applications where linear approximations can be used. To this end, several methods to linearize the Hill function (12) introduced in Section 2.3 have been considered, as further explained in Section 3.5.

In the context of anesthesia, uncertainty as a result of modeling from data may be relatively small compared to the uncertainty introduced by the use and purpose of the modeling: controlling anesthesia for all patients within a target population. Inter-patient variability in the response to anesthetic drug infusion is large and demographics cannot explain this variability (see Section 2.6). Intra-operative cardiovascular changes, co-morbidities, drug interactions and genetics also contribute to this variability. Since these are unknown prior to use of a closed-loop system, the controller cannot be designed for the individual characteristics prior to the start of anesthesia. Consequently, uncertainty descriptions suitable for controller synthesis are required. Such descriptions are the topics of Section 3.4.

Limited excitation in admissible identification data constitutes another confounding factor. Manipulating drug infusion to evoke a physiological response merely for the sake of modeling is associated with safety and ethical concerns. This limits clinical experimental conditions to those associated with providing adequate therapy. During both manual and closed-loop induction of clinical anesthesia, excitation is similar to a step reference change. Representative infusion profiles for both cases are shown in Figure 5.

Useful excitation being limited to essentially a step limits the number of identifiable parameters [Ljung, 1999]. The situation is further complicated by the presence of unmeasurable disturbances and measurement noise (see Section 3.6). Modeling and identification strategies taking the above

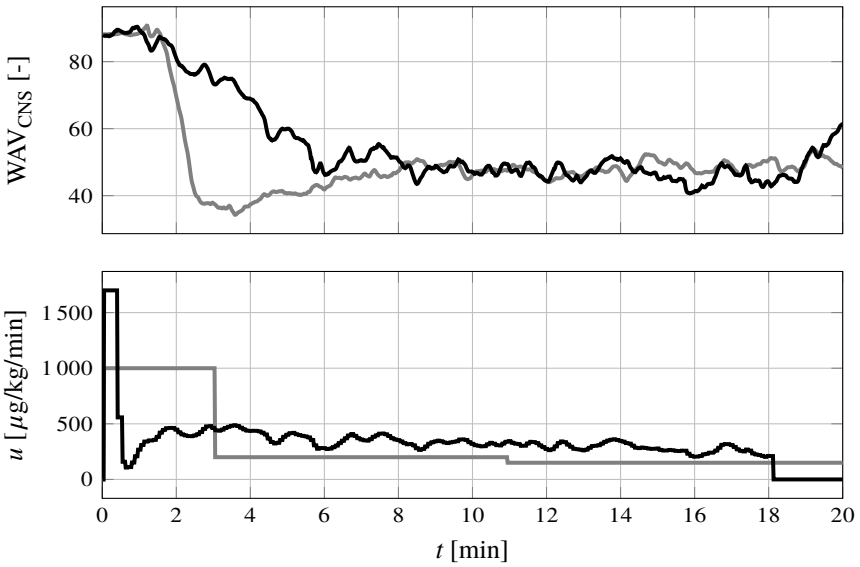

Fixa den okända referensen!

Figure 5 Representative clinical induction profiles from one manually administered case (gray) and one closed-loop controlled case (black). Top pane shows measured DoH using the NeuroSense WAV$_{CNS}$ monitor; bottom pane shows propofol infusion profiles, u. The figure is based on data previously published in [AAnonymous, 2019].

into account are the topic of Section 3.3.

The remainder of this sections is disposed as follows: methods to linearize the PD are discussed in Section 3.5; properties of clinical data, relevant to modeling, are reviewed in Section 3.2; models for control are introduced in Section 3.3. Patient variability is the topic of Section 3.4, and the section is concluded with a discussion on equipment, disturbance and noise models in Section 3.6.

3.2 Clinical data

Data quality Models for clinical pharmacology, as described in Section 2, are commonly identified from data collected in volunteer studies. For PK modeling, blood samples need to be collected and for PKPD modeling the clinical endpoint needs to be measured. These studies provide detailed information, but usually for a small number of volunteers and for a limited target population.

In contrast, models for control only require a description of the input–output behavior. Drug concentrations in the blood are not necessarily required. Any clinical endpoint (output) used for closed-loop control will be easier to measure, and provide a measurement at a higher frequency. For identification of input–output models for control, data collected during clinical practice can potentially be used, offering information on a higher number of subjects and target populations including vulnerable patients. The trade-off is the limitation on the experimental conditions.

Examples of typical time series data of propofol infusion and DoH measurements collected during clinical anesthesia are shown in Figure 5. The presence of unmeasurable disturbances from foremost surgical stimulation, combined with low signal-to-noise ratio during the maintenance phase of anesthesia (further detailed in Section 3.6), results in induction phase data being the best option for identification from representative clinical data.

Identifiability Analysis of identifiability for linear models is well established [Ljung, 1999] and persistence of excitation can be evaluated for individual data sets. For nonlinear systems, evaluation of data quality is less straightforward and excitation requirements depend on the model structure and the nonlinearity. The traditional PKPD model structure includes linear dynamics followed by a static nonlinearity, constituting a Wiener model.

Local identifiability of a nonlinear PKPD model, with realistic (step reference) excitation has been investigated through sensitivity analysis [da Silva et al., 2014]. A two-input one-output model was considered, where the inputs were propofol and remifentanil infusion and the output the measured DoH. A response surface model following the structure proposed by [Minto et al., 2000] introduces

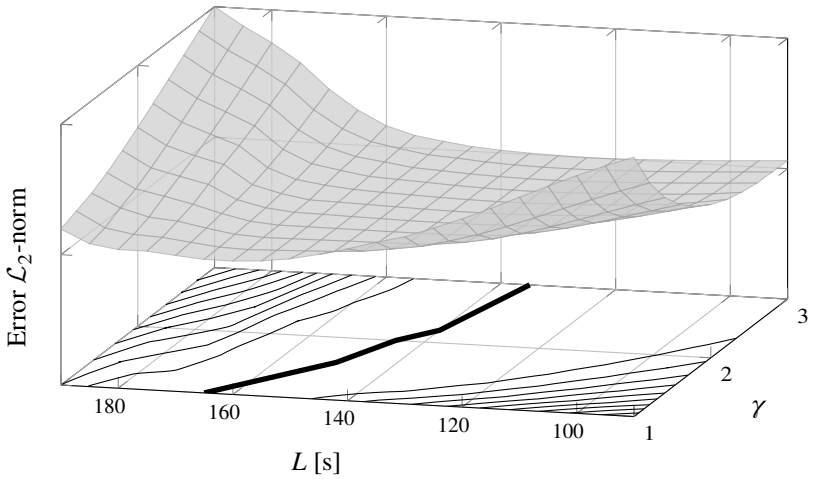

Figure 6 Model output error $\mathcal{L}_2$-norm as a function of varying the delay L and Hill function (12) parameter of the PD. Notice the flat valley in which the minimum lies (along the thick black line). A version of the figure has previously been published in [Soltesz, 2013].

the nonlinearity. Not surprisingly, this analysis indicated that this two-drug model may not be identifiable from clinical data [da Silva et al., 2014]. Identifiability of two compartmental PK models (one for each drug) and linear PD dynamics may not be guaranteed from clinical data either. When multiple clinical effects are measured for the same drug, with different PD characteristics, identifiability of PKPD parameters has been shown to improve [Kim et al., 2015]. This method has not been applied to intravenous anesthesia and identifiability results may not extend to clinical practice where excitation is limited.

When considering a PD structure with an effect-model including a time delay L (introduced below in Section 3.3), distinguishing the effect of the Hill function γ-parameter (12) from the delay is often not possible. Figure 6 shows how the $\mathcal{L}_2$ (RMS) output error of an identified PD model changes when varying the delay L and the Hill parameter γ. The surface was generated using representative induction profile data from the study underlying [van Heusden et al., 2013]. The flat valley visible in the contour plot indicates a lack of simultanous identifiability. Consequently, the approach in [van Heusden et al., 2013] was to favor over-estimation of L, to facilitate closed-loop robustness.

In addition to limited excitation, identification from clinical data is challenging due to unmeasured disturbances. In volunteer studies, the clinical environment is generally well controlled. The study protocol can include multiple drug infusion or reference changes, and nociceptive stimulation can be controlled, for example to standardized disturbances such as airway manipulation or tetanic stimulation. The timing of disturbances is therefore known, and the level is standardized. In contrast, in clinical practice, nociceptive stimulation as a result of the procedure is unpredictable and varying in intensity. Some procedures, such as airway manipulation and incision, have inspired the establishment of standardized disturbance profiles, presented in Section 3.6. However, in the clinical environment stimulation is not limited to these procedures.

Figure 7 shows examples of the effect of surgical stimulation during anesthesia. The propofol effect-site concentration C_e (filtered propofol infusion profile) indicates the average drug infusion. In example A, the DoH shows a response to airway manipulation, reflected in the increased DoH, lasting for ≈ 1 minute. The corresponding rise in heart rate indicates this was associated with a nociceptive response. The closed-loop propofol control system increased the propofol infusion accordingly, as reflected in the consequent increase in propofol C_e. During maintenance of anesthesia in the case shown in example B, some patient movement was reported. These responses to stimulation are reflected in the DoH variability and rapid DoH increases. During this period, the blood pressure was elevated. The disturbance observed in example C is of a different nature and corresponds to sustained stimulation. As a result of small changes in the DoH, the closed-loop controlled propofol infusion increases, doubling the predicted C_e during about 15 minutes. The blood pressure shows an increase during this same period, indicating a nociceptive response. Both the propofol C_e and blood pressure decrease with a presumed consequent decrease of the level of stimulation.

Disturbances due to stimulation are not zero mean, and will introduce identification bias when

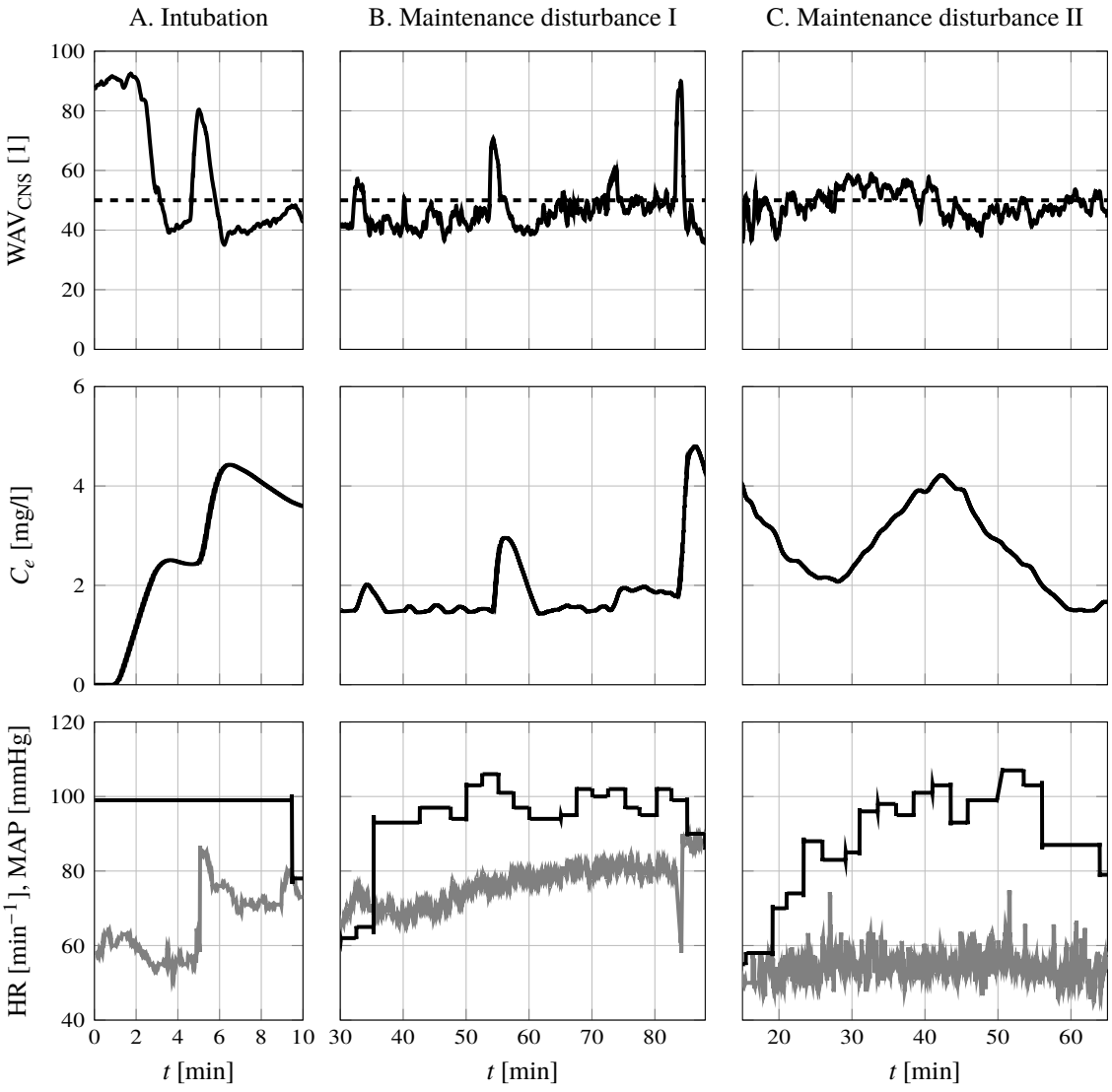

Figure 7 DoH measured with NeuroSense monitor (top, solid) and associated set-point (top, dashed); predicted propofol effect site concentration, C_e, (middle); mean arterial blood pressure measured with cuff (bottom, black) and heart rate (bottom, gray). The three columns, each from individual surgeries, represent: representative intubation disturbance during induction of anesthesia (left); distinct maintenance phase disturbances due to surgical stimulation (middle); slow maintenance phase disturbance (right). Data from closed-loop controlled study [West et al., 2018].

not taken into account. Identification of a disturbance model has consequently been proposed in [Derighetti et al., 1997], as well as multi-input single-output (MISO) and multi-input multi-output (MIMO) modeling that takes both drug administration and disturbances into account [Yelneedi et al., 2009; Lin et al., 2004; van Heusden et al., 2018c; van Heusden et al., 2017].

Data collected during closed-loop anesthesia may provide valuable information for continuing controller design, optimization and modeling for safety and verification purposes. While closed-loop identification can improve performance of model-based designs [Hjalmarsson et al., 1996], the closed-loop nature of the experiment needs to be taken into account in the identification stage. When the system input is updated based on feedback from noisy measurement, the noise in the input and output signals is correlated and standard identification methods may no longer provide unbiased estimates. Relatedly, it has been shown that when identifying the effect of propofol anesthesia on the DoH with a reduced-order model with fixed PK pre-filter, the signal-to-noise ratio is small and bias introduced by open-loop identification methods is limited [van Heusden et al., 2018c; van Heusden

et al., 2017].

3.3 Models for closed-loop anesthesia

Closed-loop anesthesia has developed into a research field of its own, involving a variation of constellations of control systems engineers and anesthesiologists. As a consequence, several models for control have been proposed. Below, a few snapshot of such models are provided, ranging from direct adaptation of pre-existing pharmacological PKPD models, to the introduction of new model structures, to enable online identifiability in the clinical context. The purpose here is to highlight different paradigms of modeling and identification, rather than to present an exhaustive list of published models for control.

Models from clinical pharmacology Models used in clinical pharmacology, introduced in Section 2, have been used for controller design and evaluation. As an example, the Schnider model for propofol [Schnider et al., 1998] and the Minto model for remifentanil [Minto et al., 1997] have been combined with an interaction model to evaluate a MISO predictive control system [Ionescu et al., 2011a]. Population average models were used, while variability was introduced by considering a population of 24 patients with randomly generated demographics. This introduces some variability in the dynamics of the PK model. However, the PD model was fixed for all patients, largely determining the lag and gain of all patient models.

In a simulation comparing four control strategies [Yelneedi et al., 2009], a large set of models was derived from the Marsh model [Marsh et al., 1991]. The Marsh model was combined with a PD model consisting of a first-order lag and Hill equation. The nominal PK parameters correspond to a 34 year old patient weighing 66 kg, and nominal PD parameters were derived from [Schnider et al., 1999] and [Sartori et al., 2006] ($k_{e0} = 0.349$ min^{-1}, $C_{e,50} = 2.65$ μg/mL, $\gamma = 2.561$; see Section 2 for details).

A variation of 25 % was assumed on the PK parameters, and a range was defined for the PD parameters based on published PKPD studies. In a first step, minimal, average and maximal values were defined for all PK parameters within the 25 % variation. Closed-loop simulations with an MPC controller over $3^8 = 6561$ models showed little effect on closed-loop performance as a result of varying volumes. In the next step, the three volume parameters were kept constant and simulations for the remaining $3^5 = 243$ models showed a small range in the achieved controller performance. Six models were selected that spanned the observed range of controller performance. PD parameters were varied at three levels for these 6 PK models resulting in $6 \cdot 3^3 = 162$ models. Closed-loop simulations with an MPC controller were performed and 17 of the 162 models were selected to cover the observed range of achieved controller performance. Model parameters for these 17 models were published [Yelneedi et al., 2009] and have subsequently been used in other studies, for example [Ionescu et al., 2011c].

Models from clinical pharmacology with identified nonlinearity Struys et al. [Struys et al., 2004] published a set of 10 virtual patients derived from the Schnider model [Schnider et al., 1998] for propofol anesthesia, used in a virtual patient simulation that allows for hardware-in-the-loop testing. The simulator included a delay to mimic the BIS delay, zero mean random noise with standard deviation of 3 BIS units and a disturbance profile that offset the BIS. The 10 virtual patient models consisted of the population average Schnider PK model, a fixed k_{e0} and Hill curve parameter, γ, (see Section 2.3), identified from clinical data collected during induction of anesthesia. These parameters were identified with a "Hill curve estimator" that was part of a closed-loop controller, evaluated for 20 female patients (18–60 years old, ASA[1] I and II) [Struys et al., 2001].

A similar strategy was adopted in [Nascu et al., 2012], disclosing a set of 12 models that combine population average PKPD dynamics with randomly generated demographics and Hill curve characteristics. Variability in the Hill curve characteristics was based on clinical insight, with no further details given. Population average PKPD dynamics were combined with Hill parameters identified from clinical data collected during induction of anesthesia by [Torrico et al., 2007]. Details on the patient population are not given.

In [Torrico et al., 2007], $E_{\max}$ was estimated from data in addition to $C_{e,50}$, E_0 and γ. The parameterization assumes that 'E_0 denotes the baseline [...] and $E_0 - -E_{\max}$ denotes the minimum achievable

[1] ASA is a physical status classification score, ranging I-VI, and provided by the American society of anesthesiologists through www.asahq.org (accessed May 4, 2019).

BIS". Below, reported values have been scaled to conform with the definitions used throughout the chapter, and defined through (12).

Five of the identified models have $E_{\max} < 0$, and for three of these $E_{\max} < -50$. For two of the models, $C_{e,50}$ exceeds 12 μg/ml. The $E_{\max}$ values are not realistic as the DoH measurement is limited between 100–0. It was therefore noted that the validity region of these models is limited to the BIS range $40 - 100$, and that for values below 40 the models do not provide a good approximation or physical interpretation.

No model validation was presented for these nonlinear models identified from clinical data. The physiologically unrealistic parameters indicate that there may have been an identifiability issue due to limited excitation or a model-plant mismatch. Evaluation of the modeling error could clarify whether the model structure can adequately predict the measurements, or whether unrealistic values are identified to compensate for this mismatch. Such model validation has important consequences for controller design. It is important to know how realistic the variability in the model set is and for which population it can be used. Furthermore, the dynamics of these models are based on population averages and all inter-patient variability is described by the nonlinearity. Since they are identified from induction data, accurate prediction of the response to the same induction profile as observed during identification can be expected. However, the model response near a setpoint of ≈ 50 relies on the population PKPD model, with all variability captured by the gain of the identified nonlinearity. Controller design relying on linearizations of this model may not perform as expected in practice. This model set is therefore not optimal for (linear) robust controller design methods. PID design using nonlinear simulations and optimization using genetic algorithms has been proposed using this model set [Padula et al., 2017].

Population average PK with identified PD model Pharmacokinetic studies that require collection of multiple blood samples are challenging, particularly so in children. Consequently, it can be practically infeasible to obtain more than a limited number of samples for each individual [Rigby-Jones and Sneyd, 2012]. Several studies of pharmacodynamics in children have therefore used predicted plasma concentrations, for example [Rigouzzo et al., 2010; Jeleazcov et al., 2008], solving the ethical and practical issues related to blood sampling, and reducing cost by omitting drug assays [Rigby-Jones and Sneyd, 2012]. This approach does not provide physiologically meaningful PD parameters. However, accurate PK predictions are not required or indicative of the PD model fit [Coppens et al., 2011]. In clinical pharmacology, accurate predictions of plasma concentrations and parameters with physiological interpretation may be important. However, when modeling input–output behavior for controller design purposes the physiological interpretation of model parameters and even its parametrization are irrelevant, as long as the structure accommodates for the observed behavior and does not do so as a consequence of over-fitting to data.

The approach to drive a previously published population average PK model with the identification data infusion profile, u and subsequently identifying the remaining dynamics between the simulated plasma concentration, C_e and the measured clinical effect E of the identification data, was utilized in [Bibian et al., 2006a] to identify patient models for closed-loop controller design. It was suggested that (8) possibly under-models the true effect-site dynamics, and argued that the effect dynamics could possibly be of higher order. However, available $u - C_p$ profiles were not of sufficient excitation to permit identification of higher order models. As a consequence, the addition of a delay was proposed to model the combined phase loss caused by higher order dynamics:

$$G_{C_p,C_e}(s) = \frac{k_{e0}}{s + k_{e0}} e^{-sL}. \tag{17}$$

The delay captures the phase-lag of the omitted higher-order dynamics. It is a common means of implicit model-order reduction, utilized in several branches of control engineering [Skogestad, 2003], and motivated by the fundamental limitations of performance imposed by a delay in the loop-transfer [Åström and Murray, 2008].

Models including a population average PK model, an effect site model (17), and a nonlinear Hill function (12) were identified in a two-step approach. In the first step the linear model was identified. In the second step the coefficients of the Hill function were identified to improve the model fit. A comparison between identification error residuals between (8) and (17) indicated that residuals obtained with (17) were significantly smaller and their distribution whiter.

In contrast to the use of PKPD models with identified (personalized) nonlinearity, in this approach the response observed during induction of anesthesia is largely captured by the linear model.

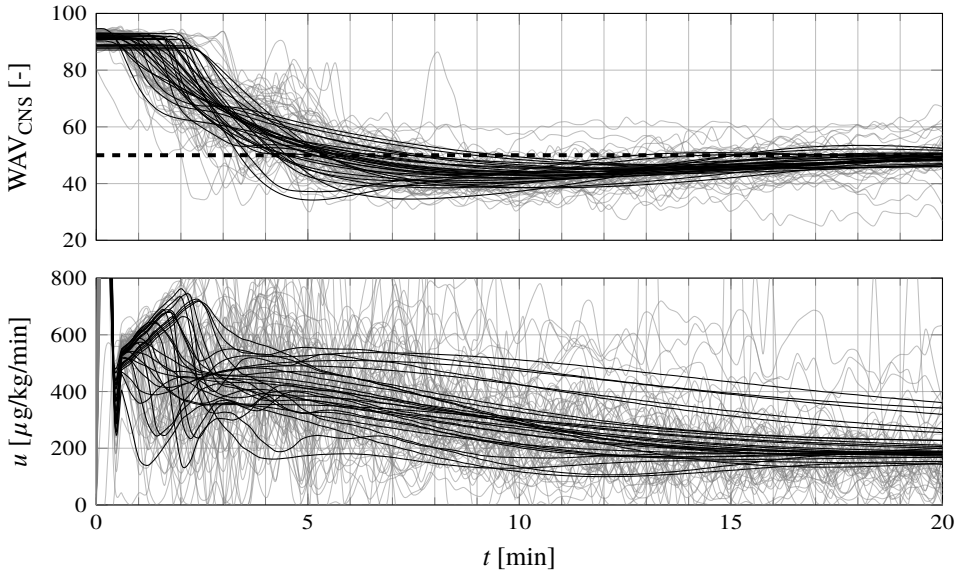

Figure 8 Comparison of predicted closed-loop response for set of 28 models (black) and 71 clinical closed-loop responses under the same controller. Top: DoH, bottom: propofol infusion. The controller was designed using this set of 28 models (gray). The comparison indicates that the performance of the design (overshoot, time to induction of anesthesia) adequately predicted performance during consequent clinical trials, the variability in the model set is realistic and the model set is control-relevant. Dashed line indicates the DoH set-point. The axis of the lower figure is cropped. The figure is generated with data previously published in [van Heusden et al., 2014].

Extrapolation of these results to drastically different induction profiles and experimental conditions is not guaranteed to yield meaningful results. However, as these models emphasize variability in the linear dynamics, they are suitable for linear controller design given the experimental conditions and closed-loop bandwidth remain similar.

When closed-loop data is available, identified linear models can improve performance of model-based designs [Hjalmarsson et al., 1996]. Models identified using this two-step approach are therefore suitable for many well-known methods for robust controller design and robustness analysis.

The described methodology, involving time-delayed effect dynamics (17), have been used in multiple subsequent studies aimed at modeling patient responses for controller design [van Heusden et al., 2013; van Heusden et al., 2018b; van Heusden et al., 2018c]. The models presented in [Bibian et al., 2006a] did not identify E_0 and may underestimate the apparent time delay. E_0 was identified in consequent studies using this approach. Several controller designs based on models identified using this methodology have been evaluated in clinical studies [van Heusden et al., 2014; van Heusden et al., 2018b; van Heusden et al., 2019]. An LTI controller was designed [van Heusden et al., 2014] based on 28 models described by [van Heusden et al., 2013], and the predicted closed-loop response in the design phase was compared to the responses observed in new cases during clinical evaluation, with the outcome shown in Figure 8 and further explained in [van Heusden et al., 2014]. The variability and overshoot of the predicted response were comparable to the measured responses [van Heusden et al., 2014], further validating the model set and modeling approach. These models also adequately predicted closed-loop responses of optimized PID control in children aged 5-10 years [van Heusden et al., 2019].

First-order models The use of a simple first-order model structure (without delay) combined with the Hill (12) nonlinearity was proposed to identify individual response models in [Hahn et al., 2012]. While PKPD models are not identifiable from clinical data, only three parameters need to be identified for this reduced-order model:

$$I_e(s) = \frac{k_e}{s + k_e} U(s), \quad E = E_0 + (E_{\max} - E_0) \frac{I_e^\gamma}{I_{50}^\gamma + I_e^\gamma}, \tag{18}$$

where $U(s)$ represents the propofol infusion, I_e is the input to the nonlinear Hill equation and the parameters k_e, I_{50} and γ remain to be identified. (Parameters E_0 and $E_{\max}$ of (18) were not used in

[Hahn et al., 2012], but have been added here to make scaling consistent throughout the chapter.)

The predictive accuracy of this model structure was compared to the accuracy achieved by a PKPD structure, for propofol anesthesia in children. Data collected during induction of anesthesia of 34 children age 6-15 years included propofol infusion rates and state entropy as measured by the M-entropy monitor (GE Healthcare, Finland). The parameters of the reduced-order model were identified using mixed-effects modeling (see Section 2.6). In the PKPD models, the PK was fixed (Paedfusor [Absalom and Kenny, 2005]) and the PD parameters were identified using mixed effects modeling. The reduced-order model achieved a lower mean square error than the PKPD structure.

While the reduced-order model structure achieved a better fit with the data, it was noted that physiologic relevance of the reduced-order models may be limited [Hahn et al., 2012]. Particularly, there is a large steady-state gain discrepancy between the structures. The infusion rates associated with stationarity at 50 % of the maximally achievable clinical effect were 110 μg/kg/min for the traditional PK model, compared to 421 μg/kg/min for the first-order model.

A first-order plus time delay (FOTD) model was considered specifically for closed-loop controller design in [van Heusden et al., 2013]. Data was available from both open-loop and closed-loop controlled induction of anesthesia in children. The clinical effect was measured by the NeuroSense monitor. For each patient, two models were identified using the two-step approach described in Section 3.3, utilizing a PK model with fixed population average parameters combined with an identified FOTD model and Hill nonlinearity, capturing the combination of PD dynamics and PK mismatch. The linear dynamics were identified in the first step. In the second step, parameters of the nonlinear Hill function were identified to improve the fit. In this study, the FOTD models also achieved a better fit than the models with PKPD structure. In addition to model validation based on residuals, the models were validated for the purpose of controller design [van Heusden et al., 2013]; the closed-loop response of each model was compared to measured closed-loop responses under the same controller. Both the published FOTD and PKPD model sets capture the observed inter-patient variability and realistically predict the response to induction of anesthesia. Bode diagrams of both model sets, shown in Figure 9, indicate that the response around the closed-loop bandwidth is similar in both model sets. As expected due to the order of the models, the high-frequency roll-off of the PKPD models is larger. The steady-state gain of the FOTD models is lower than that of the PKPD models, a property shared with the low-order models identified in [Hahn et al., 2012]. Such low-order models are therefore not appropriate for feed-forward control (TCI). However, as shown in [van Heusden et al., 2013], both the FOTD and PKPD model sets are appropriate for closed-loop controller design, where an accurate estimate of low-frequency gain is not required.

The PKPD models presented in [van Heusden et al., 2013] were subsequently used for controller design [van Heusden et al., 2014]. While both the FOTD and PKPD model sets were validated for controller design, the PKPD model set was used for two reasons: 1) due to the more realistic steady-state gain, simulated infusion rates will be more realistic; 2) in the PKPD model predicted plasma concentrations are available, providing information that can easily be interpreted by clinicians.

Application-specific reduced-order model structures To reduce the number of parameters to be identified compared to traditional PKPD models, a model structure developed specifically for modeling of anesthetic drugs was proposed in [da Silva et al., 2012]. With the notation introduced in Section 2, it is represented by

$$C_e(s) = \frac{k_1 k_2 k_3 \alpha^3}{(s+k_1\alpha)(s+k_3\alpha)(s+k_3\alpha)} U(s), \quad E = E_0 + (E_{\max} - E_0)\frac{v(t)^\gamma}{1+v(t)^\gamma}, \tag{19}$$

where $v(t) = C_e(t)/C_{e,50}$ is the normalized effect-cite concentration. The notation C_e has been used in (19) above, although no claim is made in [da Silva et al., 2012] that this entity accurately described the effect-site concentration. Rather it is referred to simply as the output of the linear portion of a Wiener model. (Parameters E_0 and $E_{\max}$ of (19) were not used in [da Silva et al., 2012], but have been added here to make scaling consistent throughout the chapter.)

The parameters k_1, k_2 and k_3, determining the ratio between the poles (located in $-k_i\alpha$) are predefined, based on prior knowledge from pharmacology of the drug at hand. The remaining parameters α, γ and $C_{e,50}$ need to be identified. The structure (19) represents higher order dynamics, while limiting the number of parameters to be identified to the same low number as for the first-order model proposed in [Hahn et al., 2012].

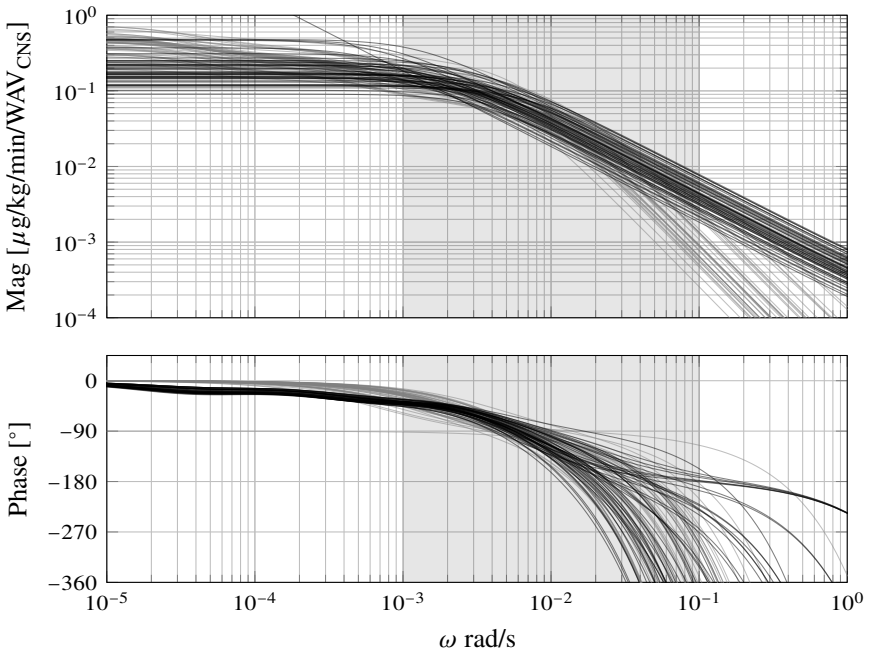

Figure 9 Bode plots of identified full PKPKD (gray) and low-order FOTD (black) models. The shaded area indicates a realistic angular frequency range for closed-loop bandwidth, based on [van Heusden et al., 2018a]. While the model sets are similar within this range, their steady-state gain differ. The models, and underlying identification procedures have been disclosed in [van Heusden et al., 2013].

In a previous simulation study, it was concluded that the parameter $C_{e,50}$ had limited effect on the identification result and $C_{e,50}$ was consequently assumed constant in [da Silva et al., 2012]. The two remaining parameters were identified using recursive identification of the nonlinear model with an extended Kalman filter, following a linearization step. In an example with clinical data, both α and γ achieved a relatively stable value after induction of anesthesia. Model validation was limited to evaluation of the residuals.

A similar MISO model structure was proposed to describe the effect of propofol and remifentanil on the depth of hypnosis in [da Silva et al., 2010]. It comprised two linear components with structure (19), respectively generating the inputs C_e^p (p for propofol) and C_e^r (r for remifentanil) to the nonlinear function

$$E = E_0 + (E_{\max} - E_0)\frac{1}{1 + \left(C_e^r(t) + mC_e^p(t)\right)^{\gamma}}, \tag{20}$$

Both $C_{e,50}^p$ and $C_{e,50}^r$ were fixed. Two linear components of the structure (19) were used; one for each drug. Their parameters, α_p and α_r, were estimated alongside m and γ, using an extended Kalman filter.

Online identification of these parameters during induction and maintenance of anesthesia did not show convergence of the parameters [da Silva et al., 2010]. For example, α changed by over 50 % during the example case. This may have been due to unmeasured disturbances, which online algorithms are generally vulnerable toward, as described in Section 3.2. The achieved model fit was adequate, but the large change in parameters over the course of induction suggest the need of additional safety measures prior to possible clinical introduction of the method.

Online identification and adaptive methods The modeling strategy discussed in Section 3.3 has been implemented online as part of a closed-loop controlled system [Struys et al., 2001]. In this system, drug infusion was updated using TCI. Induction of anesthesia was performed using a predefined infusion profile. During maintenance of anesthesia, the setpoint of the TCI was adjusted based on the measured DoH, resulting in a cascaded controller structure. The desired setpoint was calculated using the inverse of the Hill curve (see Figure 10), and an online Hill-curve estimator updated this relation in real time. Derivative action was included in the controller to reduce overshoot. Disturbances due to surgical stimulation were not taken into account and no model validation step was included.

Online identification of a propofol effect model has been proposed using Kalman filtering for use in an advisory system (prediction) [Sartori et al., 2006]. The goal of online identification was to improve the predictions. The PK model was fixed, and in addition to the states of the PK and PD model, the individual $C_{e,50}$ and k_{e0} were estimated. For 40 cases used for testing, the estimation converged. Prediction performance was significantly increased compared to predictions of a population average model.

Model-predictive control based on a PKPD model with individualized PD parameter estimates has been evaluated in a clinical trial including 80 closed-loop controlled cases [Sawaguchi et al., 2008]. A time delay L was included in the PD model, and E_0, L, $C_{e,50}$ and γ were identified using data from induction of anesthesia, with $E_{\max} = E_0$. The estimation was based on simplified relations derived using trial and error in a preliminary data set. After the online parameter estimation the controller parameters were updated and closed-loop control was initiated. Default values, as well as upper and lower bounds, for the estimates were defined for safety purposes. It was noted that the parameter estimation generally performs well, but needs to be robust to device failure and abnormal measurements. In cases where a response to stimulation following the initial propofol bolus resulted in a measured DoH $> E_0 - 30$, default values were used for control.

Identification of the dynamic PD parameters according to the model structure described in Section 3.3 following the completion of closed-loop induction of anesthesia was proposed in [Soltesz et al., 2013]. The nonlinearity parameter γ of (12) was identified in a first step; the time delay L, lag k_{e0} and gain $C_{e,50}$ were identified in a second step. The controller was then individualized for maintenance of anesthesia using constrained optimization. Compared to a population-based controller, this approach improved the mean integral absolute error by 25 % during simulated maintenance of anesthesia for 44 patient models. This study did not take measurement noise, artifacts or stimulation into account [Soltesz et al., 2013]. All these aspect would need to be thoroughly considered, and the method would need to be extended with a means of online model validation, in order to consider clinical use.

The use of online model falsification was proposed to reduce conservatism of safety-preserving control of anesthesia [Yousefi et al., 2018]. Model falsification was originally developed for model validation for robust control [Poolla et al., 1994]. Given an a priori uncertain model description, the validation problem was reformulated as a falsification problem; a model is invalidated if it is inconsistent with the data. It therefore inherently deals with missing data and limited excitation. If the data contains insufficient information to distinguish between models, they cannot be invalidated. Falsification of models describing the effect of propofol on blood pressure in the safety system was shown to reduce the conservatism introduced by robust safety-preserving control. While this method inherently deals with limited excitation, further developments are required to account for disturbances.

3.4 Patient variability

The population approach used in (clinical) PKPD modeling aims to identify the best population average dynamics and covariates to reduce the prediction error due to inter-patient variability, see Section 2.6. Identification for control on the other hand focuses on the design of robust controllers, which requires quantification of the complete uncertainty [Gevers, 2005], including outlier behavior. Methods that estimate an uncertainty set rather than a nominal model usually consider one (time-invariant) plant, where the uncertainty is a results of under-modeling (a mismatch between the model structure and the plant characteristics), limited excitation as a result of the experimental conditions, noise effects and unmodeled nonlinearities [Gevers, 2005]. In control of anesthesia, this model-plant mismatch may be relatively small compared to the variability introduced by inter-patient variability. Modeling for control of anesthesia has therefore largely focused on quantification of this inter-patient variability, and describe a set of virtual patients.

Published sets of virtual patients describing the DoH response to propofol infusion, as described in Section 3.3, are summarized in Table 1.

These sets of virtual patients provide a multi-model uncertainty description. For certain robust LTI design procedures, a nominal model and unstructured uncertainty description is required instead. This nominal model and uncertainty description are not unique. The optimal nominal frequency response at each frequency can be determined graphically [Bibian et al., 2006b]. This leads to a non-parametric (or very high-order) model. This non-parametric model can be used for controller design directly [Soltesz et al., 2016]. If a low-order description is required, optimization can be used to find

Table 1 Summary of published sets of PKPD patient model sets, together with underlying identifiction contexts, population characteristics, model set size and key model characteristics.

Context	Population	#	Model characteristics
PKPD, clinical [Yelneedi et al., 2009]	Adults	17	Population PKPD, nominal model (34 years, 66 kg), 25 % variability in PK parameters, range of PD parameters
PKPD, identified nonlinearity [Struys et al., 2004]	Adults (Female)	10	Population average nominal model with identified Hill parameters
PKPD, identified nonlinearity [Nascu et al., 2012]	Adults	12	Population average nominal model with identified Hill parameters (reported limited range of validity)
PKPD, identified PD [Bibian et al., 2006a]	Adults	44	Population average PK model with identified PD model including time delay. For use in LTI controller design
PKPD, identified PD [van Heusden et al., 2018c]	At risk adult patients	9	Population average PK, identified PD model with time delay. This set describes the effect of propofol on DoH and blood pressure.
FOTD and PKPD, identified PD [van Heusden et al., 2013]	Children age 6-16	47	FOTD and PKPD set for the same population. For use in LTI controller design.

a low-order nominal model with the desired structure [Dumont et al., 2009]. Since the optimal non-parametric nominal model cannot completely be described by a low-order transfer function, this step introduces conservatism. A two-step approach, using the optimal non-parametric model to identify a low-order nominal model, allows for quantification of this conservatism [van Heusden et al., 2018a].

Limitations due to uncertainty The described inter-patient variability is the main motivation for closed-loop anesthesia; reducing the variability in clinical effect through the use of feedback control. A well-designed feedback controller can eliminate variability at low frequencies and drastically reduce variability within the closed-loop bandwidth.

While feedback control can reduce the effect of variability, uncertainty limits the achievable performance [Goodwin et al., 2001]. If performance requirements are low, an accurate model is not required. However, to achieve high performance, an accurate system description is required.

Performance requirements for closed-loop anesthesia are relatively low; current clinical practice corresponds to manual control. Simple PID control can therefore achieve adequate performance, despite the inter-patient uncertainty. In a comparison of PID control with higher-order model-based control for a set of pediatric virtual patients, the performance improvement achieved by the additional degrees of freedom was limited [van Heusden et al., 2018a], indicating that inter-patient variability contributes more than controller structure to the limitation of achievable closed-loop performance. To improve performance, strategies that reduce the uncertainty need to be implemented.

Reducing variability Population-based PKPD modeling used in clinical pharmacology identifies covariates to reduce uncertainty. It is therefore well known that, while patient demographics cannot explain all of the observed variability, PK and PD characteristics do depend on patient age, gender, weight etc. Dividing the virtual adult patient set in age groups reduced the uncertainty [Bibian et al., 2006b]. Allometric weight-based controller scaling improved controller performance for children aged 5-10 years [van Heusden et al., 2019].

Physiologically based PKPD modeling may better account for variability related to patient demographics. The resulting model complexity is higher than that of compartmental PKPD models, and more parameters need to be determined from data. However, these parameters do not all need to be identified at the same time and from the same data source. As the parameters describe physiological processes of drug absorption, distribution, metabolism and elimination, some can be identified independently, and aggregated data from multiple studies can be used [Abbiati et al., 2018]. More detailed descriptions of the physiological processes and anatomical features may better reflect the

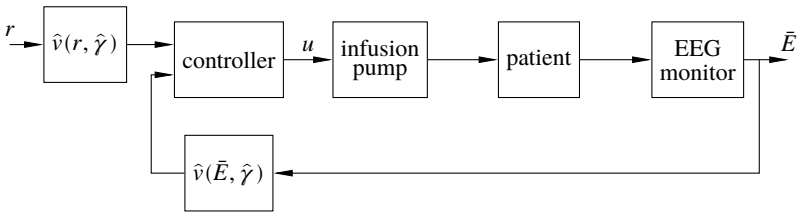

Figure 10 Block diagram showing an exactly linearizing closed-loop controller. A version of the figure has previously been published in [Soltesz, 2013].

effect of demographics on the PKPD response.

3.5 Addressing the PD nonlinearity

The PD model structure introduced in Section 2.3 contains a nonlinear component, the Hill function (12), prohibiting direct application of controller synthesis methods for LTI systemsSince the Hill function is monotone in the normalized effect-site concentration, v, it has a uniquely defined inverse

$$v(\bar{E}; \gamma) = \left(\frac{\bar{E}}{1 - \bar{E}} \right)^{1/\gamma}, \tag{21}$$

where the effect $\bar{E}$ is normalized to the inteing arval $0 - 1$. It will be used throughout this section to facilitate readability, and it can readily be achieved by applying the simple affine scaling (11) to E.

It has been suggested in [da Silva et al., 2012] and [Ionescu et al., 2008] that (21) could be implemented in the controller as illustrated by the block diagram of Figure 10. Here γ is the nonlinearity parameter of the patient, while $\hat{\gamma}$ is the parameter assumed by the controller. The strategy is termed exact linearization, as it completely cancels the nonlinearity (12) when $\hat{\gamma} = \gamma$. The exactly linearizing controller aims to control the estimated normalized drug concentration $\hat{v}(y; \hat{\gamma})$, which is straightforward, using a linear controller. Assuming that the measured and actual clinical effect are identical, i.e. $y = E$, the error in the controlled variable $\hat{v}$ becomes

$$\tilde{v} = v - \hat{v} = v - v^{\gamma/\hat{\gamma}}.$$

As further discussed in Section 3.2, clinical data is generally not sufficiently descriptive to uniquely identify γ. Consequently, exact linearization can be problematic close to the saturations $v = 0$ and $v \to \infty$ of (12), where sensitivity toward the model error $\tilde{\gamma} = \gamma - \hat{\gamma}$ is high.

Another approach, utilized by a majority of proposed and evaluated closed-loop controlled anesthesia delivery systems, is a local linearization of (12) around point $(v_w, \bar{E}_w)$:

$$\begin{aligned} \bar{E}(v) &\approx \bar{E}_w + \left. \frac{\partial \bar{E}(v; \gamma)}{\partial v} \right|_{v = v_w} \Delta V, \\ \bar{E}_w &= \bar{E}(v_w; \gamma) = 1 - \frac{1}{1 + v_w^{\gamma}}, \\ \left. \frac{\partial \bar{E}(v; \gamma)}{\partial v} \right|_{v = v_w} &= \frac{\gamma v_w^{\gamma - 1}}{(1 + v_w^{\gamma})^2}, \\ \Delta v &= v - v_w. \end{aligned} \tag{22}$$

Local linearization is performed around an equilibrium, defined by some clinical effect $\bar{E}_w$, chosen to lie close to the desired clinical effect, for example, $\bar{E}_w = 1/2$. The local and global linearization approaches coincide at $\bar{E} = \bar{E}_w$.

If the drug dosing control scheme implements integral action, it is feasible to locally model the nonlinearity as the gain $\partial \bar{E} / \partial v$. The bias term $\bar{E}_w$ of (22) is successfully compensated for by high low-frequency controller gain (introduced through for example an integrator). Particularly, the equilibrium point $(v_w = 1, \bar{E}_w = 1/2)$ yields the gain

$$\left. \frac{\partial \bar{E}}{\partial v} \right|_{v = 1} = \frac{\gamma}{4}. \tag{23}$$

When $v > 1$ it holds that

$$\frac{\gamma}{4} > \frac{\gamma v_w^{\gamma-1}}{(1+v_w^{\gamma})^2}, \qquad \forall \gamma > 0.$$

Hence (23) under-estimates the process gain when $v > 1$. In the region $0 \leq v_w \leq 1$, which is traversed during induction of anesthesia, the gain is initially zero at $E_w = 0$, whereupon it increases to reach its maximal value at

$$v_w = \left(\frac{\gamma - 1}{\gamma + 1}\right)^{1/\gamma}.$$

Assuming $\bar{E}_w = 1/2$, local linearization limits the sensitivity to errors in $\hat{\gamma}$ close to the saturations $\bar{E} = 0$ and $\bar{E} = 1$, as compared to its global counterpart. However, neither of the two strategies are particularly reliable close to the saturation, which needs to be kept in mind when synthesizing controllers for induction of anesthesia. One way to partially address the issue is to perform several local linearizations and implement a gain scheduled controller. This has been proposed in [Lin et al., 2004], where one model is used for the range $\bar{E} \leq 0.3$ and another one for $\bar{E} > 0.3$.

A third approach to handle (12) has been proposed in [Pawlowski et al., 2018], where a Smith-predictor-like [Smith, 1959] structure was introduced. This approach can be expected to have the same benefits and drawbacks that come with Smith predictors in general [Grimholt and Skogestad, 2019].

3.6 Equipment and disturbance models

All clinical monitors which perform some form of signal processing (i.e., virtually all) introduce phase lag. Phase lag – particularly caused by delay – is detrimental to closed-loop control performance and robustness. Consequently, a dynamic model of the clinical monitor is needed for controller synthesis, to guarantee properties of the resulting closed-loop system.

Measurement of neuromuscular blockage is most commonly performed through quantization of an evoked response, referred to as the train-of-four (ToF) ratio [Lee, 1975]. Apart form a known phase lag, ToF measurement is not associated with any response dynamics, which need attention in the closed-loop control context.

As opposed to neuromuscular blockage, there exists no analgesia monitor, which has enjoyed wide clinical acceptance. Due to the lack of baseline measurements (there exists no reliable gold standard), it has not been possible to identify reliable dynamic models for the commercially available units.

For hypnosis, there exist several commercially available clinical monitors. The Bispectral index is the most widely known and employed one. Others include the previously mentioned M-Entropy and NeuroSense monitors.

Most clinical EEG monitors utilize proprietary filtering, yielding a time-varying delay in their response dynamics. For instance, identified delays ranging 14–155 s have been reported for the BIS monitor [Pilge et al., 2006]. This can have severe implications on the robustness, or even stability, of a closed-loop system. One approach to mitigate the effect (provided that the delay is unknown as a consequence of a proprietary filtering algorithm), is to identify the delay online [Ionescu et al., 2011b].

Unlike the BIS and similar monitors, the NeuroSense was engineered with closed-loop control in mind. It has linear and time-invariant (LTI) response dynamics, relating measured effect, y to actual effect E:

$$G_{y,E}(s) = M(s) = \frac{1}{(8s+1)^2},$$

where the time constant is given in seconds.

Despite the mentioned filtering, there remains noise in the measured clinical effect. It can be modeled as an additive disturbance, n, entering the system at the same point as surgical disturbances, as illustrated in Figure 11. For the NeuroSense monitor, spectral analysis has revealed that n is essentially a band-limited white signal, where the band limit is imposted by the 1 Hz sampling frequency of the monitor [Soltesz, 2013]. Admissible closed-loop bandwidth is limited by the PKPD of propofol to a an order of magnitude less than the noise bandwidth, allowing for additional low-pass filtering in the feedback controller.

Modern infusion pumps typically have a linear dynamic response within the bandwidth of relevance to closed-loop controlled anesthesia (up to 1 Hz). Quantization is generally not a concern, and its effect can be mitigated by using a more diluted drug solution. There is typically a small delay

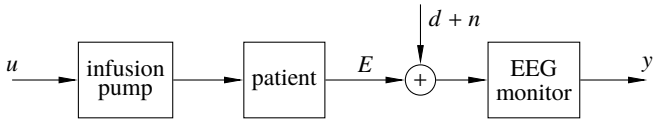

Figure 11 Block diagram illustrating the path through which surgical stimulation, d, and measurement noise, n, affects the measured clinical effect, y.

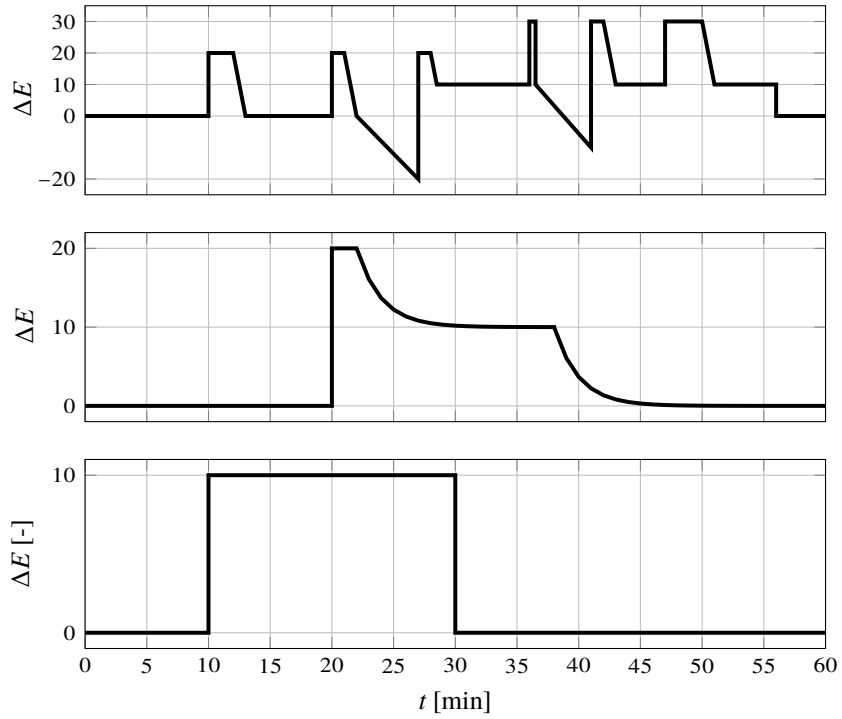

Figure 12 Additive output disturbance profiles, modeling the effect of surgical stimulation on hypnotic depth. Definitions of the profiles (top to bottom) were originally published in [Struys et al., 2004], [Dumont et al., 2009] and [Soltesz, 2013].

(tens of ms) between remotely issuing an infusion command, and a pump responding. Most pumps, which allow remote control, also have a maximal control signal update frequency (tens of Hz). Consequently, it is generally sufficient to model the actuator as a series connection of a (short) delay and a zero-order-hold circuit. The latter could alternatively be considered as part of the controller model.

Feedback controllers in anesthesia are foremost addressing the regulator (disturbance attenuation) problem. The most notable disturbances are those caused by surgical and other nociceptive stimulation, and acting on the awareness level. They enter the system at the patient input.

For example, events such as intubation or incision during the induction phase of anesthesia typically decrease the effect of hypnotic drugs. The same holds true for surgical stimulation throughout the maintenance phase. It is typically not possible to measure (or predict) such disturbances, and consequently not possible to counteract them pro-actively using feed-forward control. A feedback controller for the hypnotic component of anesthesia must therefore attenuate these disturbances sufficiently to avoid adverse effects, such as sudden hemodynamic changes or awareness.

A first step in ensuring sufficient disturbance attenuation, is to know the characteristics of the expected disturbances. To this end, a few disturbance models have been proposed in the literature [Struys et al., 2004; Dumont et al., 2009; Soltesz, 2013]. They are largely similar in that they all assume an additive disturbance, acting on the clinical effect, as illustrated in Figure 11. Furthermore, they all model the disturbance resulting from stimulation as steps or similar slowly changing signals, illustrated in Figure 12. Clinical data sets with representative such disturbances are shown in Figure 7.

Acknowledgements

The authors would like to acknowledge Dr. J. Mark Ansermino, other members of the pediatric anesthesia research team at BC Childrens Hospital (Vancouver, Canada) as well as researchers with the Department of Electrical and Computer Engineering at the University of British Columbia (Vancouver, Canada) for contributions to works upon which parts of this chapter are based; The Linnaeus Center for Control of Complex Engineering Systems at Lund University (Lund, Sweden) for funding the involvement of the author Kristian Soltesz in work underlying this chapter; Leif Andersson with the Department of Automatic Control at Lund University (Lund, Sweden) for help with figures and typesetting.

References

AAnonymous, A. (2019). "An unknown article". *Nature* **5**:4.

Abbiati, R., A. Savoca, and D. Manca (2018). "An engineering oriented approach to physiologically based pharmacokinetic and pharmacodynamic modeling". In: *Computer aided chemical engineering*. Vol. 42, pp. 37–63. DOI: 10.1016/B978-0-444-63964-6.00002-7.

Absalom, A. and G. Kenny (2005). "Paedfusor pharmacokinetic data set". *Bristish journal of anaestesia* **95**:1, pp. 110–113. DOI: 10.1093/bja/aei567.

Absalom, A. and M. Kiera (2017). *Total intravenous anesthesia and target controlled infusions. Comprehensive global anthology*. Springer, Cham, Switzerland. ISBN: 978-3319476070.

Absalom, A., V. Mani, T. De Smet, and M. Struys (2009). "Pharmacokinetic models for propofol—defining and illuminating the devil in the detail". *British journal of anaesthesia* **103**:1, pp. 26–37. DOI: 10.1093/bja/aep143.

Absalom, A. and M. Struys (2007). *An overview of TCI & TIVA*. Lannoo, Tielt, Belgium. ISBN: 978-9038211077.

Åström, K. J. and R. Murray (2008). *Feedback systems. An introduction for scientists and engineers*. Princeton university press, Princeton, NJ. ISBN: 978-0691135762.

Bibian, S. (2006). *Automation in Clinical Anesthesia*. PhD thesis. University of British Columbia, Vancouver, Canada.

Bibian, S., G. Dumont, M. Huzmezan, and C. Ries (2006a). "Patient variability and uncertainty quantification in anesthesia: part I–PKPD modeling and identification". *IFAC Proceedings volumes* **39**:18, pp. 549–554. DOI: 10.3182/20060920-3-FR-2912.00097.

Bibian, S., G. Dumont, M. Huzmezan, and C. Ries (2006b). "Patient variability and uncertainty quantification in anesthesia: part II–PKPD uncertainty". *IFAC Proceedings volumes* **39**:18, pp. 555–560. DOI: 10.3182/20060920-3-FR-2912.00097.

Bouillon, T., J. Bruhn, L. L. Radu-Radulescu, E. Bertaccini, S. Park, and S. Shafer (2002). "Non-steady state analysis of the pharmacokinetic interaction between propofol and remifentanil". *Anesthesiology* **97**:6, pp. 1350–1362. DOI: 10.1097/00000542-200212000-00005.

Bryson, H., B. Fulton, and D. Faulds (1995). "Propofol". *Drugs* **50**:3, pp. 513–559. DOI: 10.2165/00003495-199550030-00008.

Chevalier, A., D. Copot, C. Ionescu, J. Machado, and R. De Keyser (2014). "Discontinuity and complexity in nonlinear physical systems". In: Machado, J. et al. (Eds.). Springer, Cham, Switzerland. Chap. Emerging tools for quantifying unconscious analgesia: fractional-order impedance models, pp. 135–149. ISBN: 978-3-319-01411-1. DOI: 10.1007/978-3-319-01411-1_8.

Choo, E., W. Magruder, C. Montgomery, J. Lim, R. Brand, and M. Ansermino (2010). "Skin conductance fluctuations correlate poorly with postoperative self-report pain measures in school-aged children". *Anesthesiology* **113**:1, pp. 175–182. DOI: 10.1093/bja/aeg178.

Coppens, M., D. Eleveld, J. Proost, L. Marks, J. Van Bocxlaer, H. Vereecke, A. Absalom, and M. Struys (2011). "An evaluation of using population pharmacokinetic models to estimate pharmacodynamic parameters for propofol and bispectral index in children". *Anesthesiology* **115**:1, pp. 83–93. DOI: 10.1097/ALN.0b013e31821a8d80.

Cortinez, L. (2014). "What is the k_{e0} and what does it tell me about propofol?" *Anaesthesia* **69**:5, pp. 399–402. DOI: 10.1111/anae.12642.

Cortinez, L., B. Anderson, A. Penna, L. Olivares, H. Munoz, N. Holford, M. Struys, and P. Sepulveda (2010). "Influence of obesity on propofol pharmacokinetics: derivation of a pharmacokinetic model". *British journal of anaesthesia* **105**:4, pp. 448–456. DOI: 10.1093/bja/aeq195.

Cortínez, L., N. De la Fuente, D. Eleveld, A. Oliveros, F. Crovari, P. Sepulveda, M. Ibacache, and S. Solari (2014). "Performance of propofol target-controlled infusion models in the obese: pharmacokinetic and pharmacodynamic analysis". *Anesthesia & analgesia* **119**:2, pp. 302–310. DOI: 10.1213/ANE.0000000000000317.

da Silva, M., J. Lemos, A. Coito, B. Costa, T. Wigren, and T. Mendonça (2014). "Local identifiability and sensitivity analysis of neuromuscular blockade and depth of hypnosis models". *Computer methods and programs in biomedicine* **113**:1, pp. 23–36. DOI: 10.1016/j.cmpb.2013.07.020.

da Silva, M., T. Mendonça, and T. Wigren (2010). "Online nonlinear identification of the effect of drugs in anaesthesia using a minimal parameterization and bis measurements". In: *Proceedings of the 2010 American control conference*. Baltimore, MD, pp. 4379–4384. DOI: 10.1109/ACC.2010.5530791.

da Silva, M., T. Wigren, and T. Mendonça (2012). "Nonlinear identification of a minimal neuromuscular blockade model in anesthesia". *IEEE Transactions on control systems technology* **20**:1, pp. 181–188. DOI: 10.1109/TCST.2011.2107742.

Derendorf, H. and B. Meibohm (1999). "Modeling of pharmacokinetic/pharmacodynamic (PK/PD) relationships: concepts and perspectives". *Pharmaceutical research* **16**:2, pp. 176–185. DOI: 10.1023/A:1011907920641.

Derighetti, M., C. Frei, M. Buob, A. Zbinden, and T. Schnider (1997). "Modeling the effect of surgical stimulation on mean arterial blood pressure". In: *Engineering in medicine and biology society*. Chicago, IL, pp. 2172–2175. DOI: 10.1109/IEMBS.1997.758786.

Diepstraten, J., V. Chidambaran, S. Sadhasivam, H. Esslinger, S. Cox, T. Inge, C. Knibbe, and A. Vinks (2012). "Propofol clearance in morbidly obese children and adolescents". *Clinical pharmacokinetics* **51**:8, pp. 543–551. DOI: 10.1007/BF03261930.

Drover, D., C. Litalien, V. Wellis, S. Shafer, and G. Hammer (2004). "Determination of the pharmacodynamic interaction of propofol and remifentanil during esophagogastroduodenoscopy in children". *Anesthesiology* **100**:6, pp. 1382–1386. DOI: 10.1097/00000542-200406000-00008.

Dumont, G., A. Martinez, and M. Andermino (2009). "Robust control of depth of anesthesia". *International journal of adaptive control and signal processing* **23**:5, pp. 435–454. DOI: 0.1002/acs.1087.

Eleveld, D., J. Proost, L. Cortínez, A. Absalom, and M. Struys (2014). "A general purpose pharmacokinetic model for propofol". *Anesthesia & analgesia* **118**:6, pp. 1221–1237. DOI: 10.1213/ANE.0000000000000165.

Gambús, P. and I. Trocóniz (2015). "Pharmacokinetic–pharmacodynamic modelling in anaesthesia". *British journal of clinical pharmacology* **79**:1, pp. 72–84. DOI: 10.1111/bcp.12286.

Gepts, E., F. Camu, I. Cockshott, and E. Douglas (1987). "Disposition of propofol administered as constant rate intravenous infusions in humans". *Anesthesia and analgesia* **66**:12, pp. 1256–1263. DOI: 10.1213/00000539-198712000-00010.

Gevers, M. (2005). "Identification for control: from the early achievements to the revival of experiment design". *European journal of control* **11**:4–5, pp. 335–352. DOI: 10.3166/ejc.11.335-352.

Goodwin, G., S. Graebe, and M. Salgado (2001). *Control system design*. Prentice Hall, Upper Saddle River, NJ. ISBN: 978-0139586538.

Grimholt, C. and S. Skogestad (2019). "Should we forget the Smith predictor?" *IFAC-PapersOnLine* **51**:4, pp. 769–774. DOI: 10.1016/j.ifacol.2018.06.203.

Gruenewald, M. and C. Ilies (2013). "Monitoring the nociception–anti-nociception balance". *Best practice & research clinical anesthesiology* **27**:2, pp. 235–247. DOI: 10.1016/j.bpa.2013.06.007.

Guignard, B. (2006). "Monitoring analgesia". *Best practice & research clinical anaesthesiology* **22**, pp. 161–180. DOI: 10.1016/j.bpa.2005.09.002.

Hahn, J.-O., G. Dumont, and M. Ansermino (2012). "A direct dynamic dose-response model of propofol for individualized anesthesia care". *Transactions on biomedical engineering* **59**:2, pp. 571–578. DOI: 10.1109/TBME.2011.2179033.

Hara, M., K. Masui, D. Eleveld, M. Struys, and O. Uchida (2017). "Predictive performance of eleven pharmacokinetic models for propofol infusion in children for long-duration anaesthesia". *British journal of anaesthesia* **118**:3, pp. 415–423. DOI: 10.1093/bja/aex007.

Heeremans, E., J. Proost, D. Eleveld, A. Absalom, and M. Struys (2010). "Population pharmacokinetics and pharmacodynamics in anesthesia, intensive care and pain medicine". *Current opinion in anesthesiology* **23**:4, pp. 479–484. DOI: 10.1097/ACO.0b013e32833a1d2.

Hemmerling, T., S. Charabati, E. Salhab, D. Bracco, and P.-. Mathieu (2009). "The analgoscore: a novel score to monitor intraoperative nociception and its use for closed-loop application of remifentanil". *Journal of computers* **4** (4), pp. 311–318. DOI: 10.4304/jcp.4.4.311-318.

Hjalmarsson, H. (2005). "From experiment design to closed-loop control". *Automatica* **41**:3, pp. 393–438. DOI: 10.1016/j.automatica.2004.11.021.

Hjalmarsson, H., M. Gevers, and F. De Bruyne (1996). "For model-based control design, closed-loop identification gives better performance". *Automatica* **32**:12, pp. 1659–1673. DOI: 10.1016/S0005-1098(96)80003-3.

Huiku, M., K. Uutela, M. van Gils, I. Korhonnen, M. Kymäläinen, P. Meriläinen, M. Paloheimo, M. Rantanen, P. Takala, H. Viertiö-Oja, and A. Yli-Hankala (2007). "Assessment of surgical stress during general anaesthesia". *British journal of anaesthesia* **98**:4, pp. 447–455. DOI: 10.1093/bja/aem004.

Ionescu, C., R. de Keyser, C. Bismark, T. De Smet, and J. Struys M. Normey-Rico (2008). "Robust predictive control strategy applied for propofol dosing using BIS as controlled variable during anesthesia". *IEEE Transactions on biomedical engineering* **55**:9, pp. 2161–2170. DOI: 10.1109/TBME.2008.923142.

Ionescu, C., R. De Keyser, and M. Struys (2011a). "Evaluation of a propofol and remifentanil interaction model for predictive control of anesthesia induction". In: *IEEE Conference on decision and control and European control conference*. Orlando, FL, pp. 7374–7379. DOI: 10.1109/CDC.2011.6160404.

Ionescu, C., R. Hodrea, and R. De Keyser (2011b). "Variable time-delay estimation for anesthesia control during intensive care". *IEEE Transactions on biomedical engineering* **58**:2, pp. 363–369. DOI: 10.1109/TBME.2010.2088121.

Ionescu, C., A. Lopes, D. Copot, J. Machado, and J. Bates (2017). "The role of fractional calculus in modeling biological phenomena: a review". *Communications in nonlinear science and numerical simulation* **51**, pp. 141–159. DOI: 10.1016/j.cnsns.2017.04.001.

Ionescu, C., I. Nascu, and R. De Keyser (2011c). "Robustness tests of a model based predictive control strategy for depth of anesthesia regulation in a propofol to bispectral index framework". In: *International conference on advancements of medicine and health care through technology*. Cluj-Napoca, Romania, pp. 234–239. DOI: 10.1007/978-3-642-22586-4_50.

Jeanne, M., R. Logier, J. De Jonckheere, and B. Tavernier (2009). "Heart rate variability during total intravenous anesthesia: effects of nociception and analgesia". *Autonomic neuroscience* **147**:1–2, pp. 91–96. DOI: 10.1016/j.autneu.2009.01.005.

Jeleazcov, C., H. Ihmsen, J. Schmidt, C. Ammon, H. Schwilden, J. Schüttler, and J. Fechner (2008). "Pharmacodynamic modelling of the bispectral index response to propofol-based anaesthesia during general surgery in children". *British journal of anaesthesia* **100**:4, pp. 509–516. DOI: 10.1093/bja/aem408.

Kern, S., G. Xie, J. White, and T. Egan (2004). "Opioid-hypnotic synergy: a response surface analysis of propofol-remifentanil pharmacodynamic interaction in volunteers". *Anesthesiology* **100**:6, pp. 1374–1381.

Kim, C.-S., N. Fazeli, and J.-O. Hahn (2015). "Data-driven modeling of pharmacological systems using endpoint information fusion". *Computers in biology and medicine* **61**, pp. 36–47. DOI: 10.1016/j.compbiomed.2015.03.010.

Le Guien M. Liu, N., T. Chazot, and M. Fischler (2016). "Closed-loop anesthesia". *Minerva Anestesiologica* **82**:5, pp. 573–581.

Lee, C. (1975). "Train-of-4 quantitation of competitive neuromuscular block". *Anesthesia & analgesia* **54**:5, pp. 649–653. DOI: 10.1213/00000539-197509000-00021.

Lee, W., B. Anderson, R. Kosut, and I. Mareels (1993). "A new approach to adaptive robust control". *International journal of adaptive control and signal processing* **7**:3, pp. 183–211. DOI: 10.1002/acs.4480070303.

Lemmens, H. and D. Stanski (2012). "Individualized dosing with anesthetic agents". *Clinical pharmacology & therapeutics* **92**:4, pp. 417–419. DOI: 10.1038/clpt.2012.131.

Lin, H.-H., C. Beck, and M. Bloom (2004). "On the use of multivariable piecewise-linear models for predicting human response to anesthesia". *IEEE Transactions on biomedical engineering* **51**:11, pp. 1876–1887. DOI: 10.1109/TBME.2004.831541.

Ljung, L. (1999). *System identification. theory for the user*. Prentics Hall, Upper Saddle River, NJ. ISBN: 978-0136566953.

Luenberger, D. (1979). *Introduction to dynamic systems*. Wiley, Hoboken, NJ. ISBN: 0-471-02594-1.

Marsh, B., M. White, N. Morton, and G. Kenny (1991). "Pharmacokinetic model driven infusion of propofol in children". *British journal of anaesthesia* **67**:1, pp. 41–48. DOI: 10.1093/bja/67.1.41.

Mendonça, T., H. Magalhaes, P.-. Lago, and S. Esteves (2004). "Hippocrates: a robust system for the control of neuromuscular blockade". *Clinical monitoring and computing* **18**:4, pp. 265–273. DOI: 10.1007/s10877-005-2222-4.

Merigo, L., F. Padula, N. Latronico, M. Paltenghi, and A. Visioli (2019). "Optimized PID control of propofol and remifentanil coadministration for general anesthesia". *Communications in nonlinear science and numerical simulation* **72**, pp. 194–212. DOI: 10.1016/j.cnsns.2018.12.015.

Milne, S., G. Kenny, and S. Schraag (2003). "Propofol sparing effect of remifentanil using closed-loop anaesthesia". *British journal of anaesthesia* **90**, pp. 623–629. DOI: 10.1093/bja/aeg115.

Minto, C. and T. Schnider (2008). "Contributions of PK/PD modeling to intravenous anesthesia". *Clinical pharmacology & therapeutics* **84**:1, pp. 27–38. DOI: 10.1038/clpt.2008.100.

Minto, C., T. Schnider, T. Egan, E. Youngs, E. Lemmens, P. Gambus, V. Billard, J. Hoke, K. Moore, D. Hermann, K. Muir, J. Mandema, and S. Shafer (1997). "Influence of age and gender on the pharmacokinetics and pharmacodynamics of remifentanil: I. model development". *Anesthesiology* **86**:1, pp. 10–23.

Minto, C., T. Schnider, T. Short, K. Gregg, A. Gentilini, and L. Shafter (2000). "Response surface model for anesthetic drug interactions". *Anesthesiology* **92**:6, pp. 1603–1616. DOI: 10.1097\%2F00000542-200006000-00017.

Nascu, I., C. Ionescu, and R. De Keyser (2012). "Adaptive EPSAC predictive control of the hypnotic component in anesthesia". In: *Proceedings of 2012 IEEE international conference on automation, quality and testing, robotics*. Cluj-Napoca, Romania, pp. 103–108. DOI: 10.1109/AQTR.2012.6237683.

Neckebroeak, M., T. De Smet, and M. Struys (2013). "Automated drug delivery in anesthesia". *Current anesthesiology reports* **3**:1, pp. 18–26. DOI: 10.1007/s40140-012-0004-3.

Padula, F., C. Ionescu, N. Latronico, M. Paltenghi, A. Visioli, and G. Vivacqua (2017). "Optimized pid control of depth of hypnosis in anesthesia". *Computer methods and programs in biomedicine* **144**, pp. 21–35. DOI: 10.1016/j.cmpb.2017.03.013.

Pawlowski, A., L. Merigo, J. Guzmán, and S. Dormido (2018). "Two-degree-of-freedom control scheme for depth of hypnosis in anesthesia". *IFAC-PapersOnLine* **51**:4, pp. 72–77. DOI: 10.1016/j.ifacol.2018.06.034.

Pilge, S., R. Zanner, G. Schneider, J. Blum, M. Kreuzer, and E. Kochs (2006). "Time delay of index calculation: analysis of cerebral state, bispectral, and narcotrend indices". *Anesthesiology* **104**:3, pp. 488–494. DOI: 10.1097/00000542-200603000-00016.

Poolla, K., P. Khargonekar, A. Tikku, J. Krause, and K. Nagpal (1994). "A time-domain approach to model validation". *IEEE Transactions on automatic control* **39**:5, pp. 951–959. DOI: 10.1109/9.284871.

Rigby-Jones, A., M. Priston, J. Sneyd, A. McCabe, G. Davis, M. Tooley, G. Thorne, and A. Wolf (2007). "Remifentanil - midazolam sedation for paediatric patients receiving mechanical ventilation after cardiac surgery". *British journal of anaesthesia* **99**:2, pp. 252–261. DOI: 10.1093/bja/aem135.

Rigby-Jones, A. and J. Sneyd (2012). "Pharmacokinetics and pharmacodynamics–is there anything new?" *Anaesthesia* **67**:1, pp. 5–11. DOI: 10.1111/bcp.13163.

Rigouzzo, A., F. Servin, and I. Constant (2010). "Pharmacokinetic-pharmacodynamic modeling of propofol in children". *Anesthesiology* **113**:2, pp. 343–352. DOI: 10.1097/ALN.0b013e318273e272.

Roberts, F., J. Dixon, G. Lewis, R. Tackley, and C. Prys-Roberts (1988). "Induction and maintenance of propofol anaesthesia: a manual infusion scheme". *Anaesthesia* **43**, pp. 14–17. DOI: 10.1111/j.1365-2044.1988.tb09061.x.

Rugh, W. and T. Kailath (1995). *Linear system theory*. 2nd. Pearson, London, UK. ISBN: 978-0134412054.

Safonov, M. (2012). "Origins of robust control: early history and future speculations". *Annual reviews in control* **36**:2, pp. 173–181. DOI: 10.1016/j.arcontrol.2012.09.001.

Sahinovic, M., M. Struys, and A. Absalom (2018). "Clinical pharmacokinetics and pharmacodynamics of propofol". *Clinical pharmacokinetics* **57**:12, pp. 1539–1558. DOI: 10.1007/s40262-018-0672-3.

Sartori, V., P. Schumacher, T. Bouillon, M. Luginbuehl, and M. Morari (2006). "On-line estimation of propofol pharmacodynamic parameters". In: *IEEE Engineering in medicine and biology 27th annual Conference*. Shanghai, China, pp. 74–77. DOI: 10.1109/IEMBS.2005.1616345.

Sawaguchi, Y., E. Furutani, G. Shirakami, M. Araki, and K. Fukuda (2008). "A model-predictive hypnosis control system under total intravenous anesthesia". *IEEE Transactions on biomedical engineering* **55**:3, pp. 874–887. DOI: 10.1109/TBME.2008.915670.

Schnider, T., C. Minto, P. Gambus, C. Andresen, D. Goodale, S. Shafer, and E. Youngs (1998). "The influence ofd method of administration and covariates on the pharmacokinetics of propofol in adult volunteers". *Anesthesiology* **88**:5, pp. 1170–1182.

Schnider, T., C. Minto, S. Shafer, P. Gambus, C. Andresen, D. Goodale, and E. Youngs (1999). "The influence of age on propofol pharmacodynamics". *Anesthesiology* **90**:6, pp. 1502–1516. DOI: 10.1097\%2F00000542-199701000-00004.

Shafer, S. and J. Varvel (1991). "Pharmacokinetics, pharmacodynamics, and rational opioid selection". *Anesthesiology* **74**:1, pp. 53–63. DOI: 10.1097/00000542-199101000-00010.

Sheiner, L. and S. Beal (1980). "Evaluation of methods for estimating population pharmacokinetic parameters". *Pharmacokinetics and biopharmaceutics* **8**:6, pp. 553–571. DOI: 10.1007/BF01061870.

Sheiner, L., B. Rosenberg, and V. Marathe (1977). "Estimation of population characteristics of pharmacokinetic parameters from routine clinical data". *Journal of pharmacokinetics and biopharmaceutics* **5**:5, pp. 445–479. DOI: 10.1007/BF01061728.

Sheiner, L., D. Stanski, S. Vozeh, R. Miller, and J. Ham (1979). "Simultaneous modeling of pharmacokinetics and pharmacodynamics: application to D-tubocurarine". *Clinical pharmacology and therapeutics* **25**:3, pp. 358–371. DOI: 10.1002/cpt1979253358.

Skogestad, S. (2003). "Simple analytic rules for model reduction and PID controller tuning". *Journal of process control* **13**:4, pp. 291–309. DOI: 10.1016/S0959-1524(02)00062-8.

Smith, O. (1959). "A controller to overcome dead time". *ISA journal* **6**:2, pp. 28–33. DOI: 10.4236/ajps.2013.410242.

Soltero, D., A. Faulconer, and R. Bickford (1951). "The clinical application of automatic anesthesia". *Anesthesiology* **12**:5, pp. 574–582. DOI: 10.1097\%2F00000542-195109000-00004.

Soltesz, K. (2013). *On automation in anesthesia*. PhD thesis. Lund University, Lund, Sweden. ISBN: 978-91-7473-484-3.

Soltesz, K., J.-O. Hahn, T. Hägglund, G. Dumont, and M. Ansermino (2013). "Individualized closed-loop control of propofol anesthesia: a preliminary study". *Biomedical signal processing and control* **8**:6, pp. 500–508. DOI: 10.1016/j.bspc.2013.04.005.

Soltesz, K., K. van Heusden, M. Hast, M. Ansermino, and G. Dumont (2016). "A synthesis method for automatic handling of inter-patient variability in closed-loop anesthesia". In: *2016 American Control Conference*. Boston, MA, pp. 4877–4882. DOI: 10.1109/ACC.2016.7526125.

Struys, M., T. De Smet, B. Depoorter, L. Versichelen, E. Mortier, F. Dumortier, S. Shafer, and G. Rolly (2000). "Comparison of plasma compartment versus two methods for effect compartment–controlled target-controlled infusion for propofol". *Anesthesiology* **92**:2, pp. 399–399. DOI: 10.1213/00000539-198712000-00010.

Struys, M., T. De Smet, S. Greenwald, A. Absalom, S. Bingé, and E. Mortier (2004). "Performance evaluation of two published closed-loop control systems using bispectral index monitoring; a simulation study". *Anesthesiology* **100**:3, pp. 640–647. DOI: 10.1097/00000542-200403000-00026.

Struys, M., T. De Smet, L. Versichelen, S. Van de Velde, R. Van den Broecke, and E. Mortier (2001). "Comparison of closed-loop controlled administration of propofol using bispectral index as the controlled variable versus ´´standard practice" controlled administration". *Anesthesiology* **95**:1, pp. 6–17. DOI: 10.1213/ANE.0b013e318205680b.

Torrico, B., R. De Keyser, C. Ionescu, and J. Rico (2007). "Robust predictive control of drug dosing during anesthesia". In: *2007 European control conference (ECC)*. Kos, Greece, pp. 3139–3145. DOI: 10.23919/ECC.2007.7068629.

van Heusden, K., M. Ansermino, and G. Dumont (2017). "Closed-loop instrumental variable identification of propofol anesthesia". In: *2017 IEEE Conference on control technology and applications (CCTA)*. Mauna Lani, HI, pp. 1165–1170. DOI: 10.1109/CCTA.2017.8062616.

van Heusden, K., M. Ansermino, and G. Dumont (2018a). "Performance of robust PID and Q-design controllers for propofol anesthesia". *IFAC-PapersOnLine* **51**:4, pp. 78–83. DOI: 10.1016/j.ifacol.2018.06.036.

van Heusden, K., M. Ansermino, and G. Dumont (2018b). "Robust MISO control of propofol-remifentanil anesthesia guided by the NeuroSENSE monitor". *IEEE Transactions on control systems engineering* **26**:5, pp. 1758–1770. DOI: 10.1109/TCST.2017.2735359.

van Heusden, K., M. Ansermino, K. Soltesz, S. Khosravi, N. West, and G. Dumont (2013). "Quantification of the variability in response to propofol administration in children". *Transactions on biomedical engineering* **60**:9, pp. 2521–2529. DOI: 10.1109/TBME.2013.2259592.

van Heusden, K., G. Dumont, K. Soltesz, C. Petersen, A. Umedaly, N. West, and M. Ansermino (2014). "Design and clinical evaluation of robust pid control of propofol anesthesia in children". *Transactions on control systems technology* **22**:2, pp. 491–501. DOI: 10.1109/TCST.2013.2260543.

van Heusden, K., K. Soltesz, E. Cooke, S. Brodie, N. West, M. Görges, J. M. Ansermino, and G. A. Dumont (2019). "Optimizing robust PID control of propofol anesthesia for children; design and clinical evaluation". *IEEE Transactions on Biomedical Engineering* **In press**. Early access. DOI: 10.1109/TBME.2019.2898194.

van Heusden, K., M. Yousefi, M. Ansermino, and G. Dumont (2018c). "Closed-loop MISO identification of propofol effect on blood pressure and depth of hypnosis". *IEEE Transactions on control systems technology*. DOI: 10.1109/TCST.2018.2871962.

West, N., K. van Heusden, M. Görges, S. Brodie, A. Rollinson, C. L. Petersen, G. A. Dumont, J. M. Ansermino, and R. N. Merchant (2018). "Design and evaluation of a closed-loop anesthesia system with robust control and safety system". *Anesthesia & Analgesia* **127**:4, pp. 883–894.

Yelneedi, S., L. Samavedham, and G. Rangaiah (2009). "Advanced control strategies for the regulation of hypnosis with propofol". *Industrial & engineering chemistry research* **48**:8, pp. 3880–3897. DOI: 10.1021/ie800695b.

Yousefi, M., K. van Heusden, I. Mitchell, M. Ansermino, and G. Dumont (2018). "Falsified model-invariant safety-preserving control with application to closed-loop anesthesia". *IEEE Transactions on Control Systems Technology*. Early access. DOI: 10.1109/TCST.2018.2879290.

Zhanybai, T., A. Medvedev, and M. Silva (2015). "Bifurcation analysis of PID-controlled neuromuscular blockade in closed-loop anesthesia". *Journal of process control* **25**, pp. 152–163. DOI: 10.1016/j.jprocont.2014.10.006.